CHANGES IN THE DISTRIBUTION OF LOW-ENERGY TRAPPED PROTONS ASSOCIATED WITH THE APRIL 17, 1965, MAGNETIC STORM

by

A. L. Burns and S. M. Krimigis*

This work was supported in part by the Office of Naval Research under Contract No. N00014-68-A-0196-0003

Department of Physics and Astronomy
THE UNIVERSITY OF IOWA
Iowa City, Iowa

U. of Iowa 71-8

CHANGES IN THE DISTRIBUTION OF LOW-ENERGY TRAPPED PROTONS ASSOCIATED WITH THE APRIL 17, 1965, MAGNETIC STORM

by

A. L. Burns and S. M. Krimigis*

Department of Physics and Astronomy
The University of Iowa
Iowa City, Iowa 52240

March 1971

*Now at The Johns Hopkins University, Applied Physics Laboratory, Silver Spring, Maryland 20910.

UNCLASSIFIED

Security Classification

DOCUMENT CONTROL DATA - R&D

(Security classification of title, body of abstract and indexing annotation must be entered when the overall report is classified)

1. ORIGINATING ACTIVITY (Corporate author)	2a. REPORT SECURITY CLASSIFICATION
University of Iowa Department of Physics and Astronomy	UNCLASSIFIED
	2b. GROUP

3. REPORT TITLE

Changes in the Distribution of Low-Energy Trapped Protons Associated with the April 17, 1965, Magnetic Storm

4. DESCRIPTIVE NOTES (Type of report and inclusive dates)

Progress February 1971

5. AUTHOR(S) (Last name, first name, initial)

Burns, A. L. and Krimigis, S. M.

6. REPORT DATE	7a. TOTAL NO. OF PAGES	7b. NO. OF REFS
February 1971	52	18

8a. CONTRACT OR GRANT NO.	9a. ORIGINATOR'S REPORT NUMBER(S)
N000-14-68-A-0196-0003	
b. PROJECT NO.	71-8
c.	9b. OTHER REPORT NO(S) (Any other numbers that may be assigned this report)
d.	

10. AVAILABILITY/LIMITATION NOTICES

Distribution of this document is unlimited

11. SUPPLEMENTARY NOTES	12. SPONSORING MILITARY ACTIVITY
	Office of Naval Research

13. ABSTRACT

[SEE FOLLOWING PAGE]

DD FORM 1 JAN 64 1473

UNCLASSIFIED

Security Classification

14. KEY WORDS	LINK A		LINK B		LINK C	
	ROLE	WT	ROLE	WT	ROLE	WT
Low-Energy Trapped Protons Magnetic Storms Outer Radiation Zone						

INSTRUCTIONS

1. ORIGINATING ACTIVITY: Enter the name and address of the contractor, subcontractor, grantee, Department of Defense activity or other organization *(corporate author)* issuing the report.

2a. REPORT SECURITY CLASSIFICATION: Enter the overall security classification of the report. Indicate whether "Restricted Data" is included. Marking is to be in accordance with appropriate security regulations.

2b. GROUP: Automatic downgrading is specified in DoD Directive 5200.10 and Armed Forces Industrial Manual. Enter the group number. Also, when applicable, show that optional markings have been used for Group 3 and Group 4 as authorized.

3. REPORT TITLE: Enter the complete report title in all capital letters. Titles in all cases should be unclassified. If a meaningful title cannot be selected without classification, show title classification in all capitals in parenthesis immediately following the title.

4. DESCRIPTIVE NOTES: If appropriate, enter the type of report, e.g., interim, progress, summary, annual, or final. Give the inclusive dates when a specific reporting period is covered.

5. AUTHOR(S): Enter the name(s) of author(s) as shown on or in the report. Enter last name, first name, middle initial. If military, show rank and branch of service. The name of the principal author is an absolute minimum requirement.

6. REPORT DATE: Enter the date of the report as day, month, year; or month, year. If more than one date appears on the report, use date of publication.

7a. TOTAL NUMBER OF PAGES: The total page count should follow normal pagination procedures, i.e., enter the number of pages containing information.

7b. NUMBER OF REFERENCES: Enter the total number of references cited in the report.

8a. CONTRACT OR GRANT NUMBER: If appropriate, enter the applicable number of the contract or grant under which the report was written.

8b, 8c, & 8d. PROJECT NUMBER: Enter the appropriate military department identification, such as project number, subproject number, system numbers, task number, etc.

9a. ORIGINATOR'S REPORT NUMBER(S): Enter the official report number by which the document will be identified and controlled by the originating activity. This number must be unique to this report.

9b. OTHER REPORT NUMBER(S): If the report has been assigned any other report numbers *(either by the originator or by the sponsor)*, also enter this number(s).

10. AVAILABILITY/LIMITATION NOTICES: Enter any limitations on further dissemination of the report, other than those imposed by security classification, using standard statements such as:

(1) "Qualified requesters may obtain copies of this report from DDC."

(2) "Foreign announcement and dissemination of this report by DDC is not authorized."

(3) "U. S. Government agencies may obtain copies of this report directly from DDC. Other qualified DDC users shall request through _____."

(4) "U. S. military agencies may obtain copies of this report directly from DDC. Other qualified users shall request through _____."

(5) "All distribution of this report is controlled. Qualified DDC users shall request through _____."

If the report has been furnished to the Office of Technical Services, Department of Commerce, for sale to the public, indicate this fact and enter the price, if known.

11. SUPPLEMENTARY NOTES: Use for additional explanatory notes.

12. SPONSORING MILITARY ACTIVITY: Enter the name of the departmental project office or laboratory sponsoring *(paying for)* the research and development. Include address.

13. ABSTRACT: Enter an abstract giving a brief and factual summary of the document indicative of the report, even though it may also appear elsewhere in the body of the technical report. If additional space is required, a continuation sheet shall be attached.

It is highly desirable that the abstract of classified reports be unclassified. Each paragraph of the abstract shall end with an indication of the military security classification of the information in the paragraph, represented as *(TS), (S), (C), or (U)*.

There is no limitation on the length of the abstract. However, the suggested length is from 150 to 225 words.

14. KEY WORDS: Key words are technically meaningful terms or short phrases that characterize a report and may be used as index entries for cataloging the report. Key words must be selected so that no security classification is required. Identifiers, such as equipment model designation, trade name, military project code name, geographic location, may be used as key words but will be followed by an indication of technical context. The assignment of links, roles, and weights is optional.

ABSTRACT

The absolute intensity of geomagnetically trapped protons in the energy ranges $0.52 \leq E_p \leq 4.0$ Mev and $0.90 \leq E_p \leq 1.8$ Mev has been measured with the solid state proton detector on the University of Iowa low altitude (initial apogee 2502 km, perigee 527 km), high latitude (inclination 81°) satellite Injun 4 for the period March 1 to May 31, 1965. A study of the temporal variations of these fluxes associated with the April 17, 1965, magnetic storm (sc 1313 UT April 17, main phase onset ~ 0200 UT April 18) shows a general redistribution of these protons for $L \geq 2.5$ and all sampled $|\vec{B}|$ ranges, which persisted for at least 36 days after the storm.

The effect of the sudden commencement was a general depression in the intensities and a hardening of the energy spectrums, although the intensities recovered to their pre-storm level during the initial phase. The major redistribution was apparently initiated by the polar substorm which began at ~ 0620 UT on April 18, and continued long after (to 1100 UT) the substorm had subsided (~ 0800 UT). During the recovery phase a secondary peak developed in the intensity profile at $L \sim 3.5$ for 0.52 Mev protons which had no counterpart at this energy at the equator (Davis, private communication, 1971). No such peak was observed for 0.9 Mev protons. The over-all effect

of the storm on the steady-state distribution was a nonadiabatic one with an increase in intensities at $L \leqslant 3$ and a decrease at $L \geqslant 3$. The loss and/or gain of particles appears to be fractionally the same at all $|\vec{B}|$ values sampled here. The post-storm dependence of the spectral parameter E_o on L generally follows the relation $E_o \propto L^{-3}$, although the pre-storm dependence cannot be described by a simple function at all L values. The appearance of a secondary peak and the behavior of the pre-storm and post-storm spectrums are in qualitative agreement with the predictions of the bimodal diffusion model of Theodoridis et al. [1969] whereby the solar wind is the source of the observed protons.

1. INTRODUCTION

Since the discovery of the low-energy ($\sim$ 1 Mev) protons by Bame et al. [1962] and Davis and Williamson [1963], many measurements have been reported on the spatial distribution, energy spectrums, pitch-angle distributions, etc., particularly in the steady state (for a recent review see Williams [1970]). Studies of time variations, however, have been less extensive; specifically, studies of storm-associated changes reported by Davis and Williamson [1966], Brown et al. [1968], Söraas and Davis [1968] have been concerned with observations obtained near the equator. The present data have been acquired with a high-latitude low-altitude satellite and correspond to very small ($\leq 20°$) equatorial pitch angles which are not readily sampled with low-latitude spacecraft. One of the advantages of a polar-orbiting spacecraft is that several traversals of the radiation belts can be obtained while a storm is in progress, resulting in a more detailed picture of the time variations than is possible with an equatorial spacecraft. The data reported here cover the period March 1 to May 31, 1965, which includes the April 17, 1965, magnetic storm and thus extend the observations of Brown et al. [1968] to small equatorial pitch angles.

Experimental observations of such low-energy protons may be used in determining the mechanisms responsible for populating the earth's radiation belts. In particular, it will be possible to determine the presence or absence of adiabatic acceleration and/or deceleration processes and the nonadiabatic effects. Further, diffusion processes of the type that conserve μ and J, but violate Φ [Tverskoy, 1964; Nakada et al., 1965] or of the bimodal type whereby particle diffusion in L as well as energy [Theodoridis et al., 1969] may be evaluated. In addition, the importance of pitch-angle diffusion [e.g. Haerendel, 1970] can be examined with the availability of data with small equatorial pitch angles.

The present work reports changes in trapped proton fluxes in the energy intervals $0.52 \leq E_p \leq 4$ Mev and $0.90 \leq E_p \leq 1.8$ Mev with emphasis on the magnetic storm of April 17, 1965. Variations in absolute fluxes and energy spectrum are examined in several L,B intervals and the over-all flux changes are presented in B,L space contours. The general result is that redistribution of protons in the aforementioned energy ranges occurred during and after the storm, with an increase in the post-storm flux at $2.5 \leqslant L \leqslant 3$ and a decrease at $L \geqslant 3$. Adiabatic effects were apparent at some L values during the storm ($L \geqslant 3.6$ at 0.52 Mev), while the over-all nature of the event was nonadiabatic.

2. APPARATUS AND DATA SCHEME

The observations reported herein were obtained with the totally depleted gold-silicon surface barrier detector on the University of Iowa satellite Injun 4. The two proton modes, channels A and B were used in the present study. Channel A is sensitive to protons with $0.52 \leq E_p \leq 4.0$ Mev while channel B is sensitive to protons of energy $0.9 \leq E_p \leq 1.8$ Mev. The geometric factor is 0.0064 ± 0.0007 cm^2 ster. Laboratory calibrations showed that the electron counting efficiency was $< 10^{-7}$. A fuller description of the detector and calibrations is given by Burns [1968] and Krimigis and Van Allen [1967]. During the time of these observations the satellite was oriented such that the detector axis was continuously perpendicular ($\pm$ 10°) to $\vec{B}$, the local geomagnetic field vector.

The output from channels A and B are sampled once every four seconds with a duty cycle of 25%. All telemetered data from the satellite are merged with the orbit parameters $|\vec{B}|$, L and local time and then sorted into groups specified by selected intervals of $|\vec{B}|$ and L. The intervals used here are 0.1 R_e for L and 0.02 gauss for $|\vec{B}|$.

3. THE APRIL 17, 1965, MAGNETIC STORM

The magnetic storm of April 17, 1965, was characteristic of the so called 'standard type' [Akasofu, 1966] in that there was a sudden commencement, a positive initial phase, a negative main phase, and a subsequent recovery to the initial field strength. Cahill [1966] has used the Explorer 26 magnetometer data with the horizontal field data from several low latitude magnetic observatories in analyzing the effect of this magnetic storm on the earth's magnetic field. Meng and Akasofu [1967] have made a thorough study of this storm using data from many magnetic observatories. Both of these studies show that there was an asymmetric ring current around the earth during the beginning of the main phase until about 1200 UT on April 18. The data indicate that after 1200 UT on April 18 the ring current was symmetric.

Figure 1 shows the three hour K_p index (IAGA COMMISSION IV, Geophysikalisches Institut, University of Gottingen) and the D_{st} index (Sugiura and Henricks, Goddard Space Flight Center, Greenbelt, Maryland) for the month of April, 1965. The sudden commencement of the storm was observed on the earth at 1311-1314 UT on April 17 [Lincoln, 1966]. The D_{st} index shows a main-phase depression of -137γ with a subsequent recovery time of several days.

4. OBSERVATIONS

A. General Time Profile

Figures 2 and 3 show the response of channel A versus time for the month of April, 1965 for different values of L with $|\vec{B}|$ constant. These figures show that the trapped proton fluxes were approximately constant before April 17. The time dependence of the flux after April 17 is seen to be different for three different regions in L: (1) For $L \leq 2.4$ the flux is approximately constant (within statistical uncertainty) after April 17. (2) For $2.4 \leq L < 3.0$ the flux increased and was approximately constant after April 18. The increase in flux, which was L dependent, was 8×10^3 $(cm^2\text{-sec-ster})^{-1}$ for $L \sim 2.5$ and increased for larger L to 3×10^4 $(cm^2\text{-sec-ster})^{-1}$ for $2.7 \leq L < 2.8$. The increase for these two cases are about 20% and 35% respectively. (3) For $L \geq 3.0$ the flux decreased sharply on April 18. The decrease was about a factor of 2 at $3.0 \leq L < 3.1$ and became greater with increasing L such that for $L \geq 3.3$ the decrease was more than a factor of 10. The subsequent time behavior in this region was also L dependent. For $3.0 \leq L < 3.1$ the flux was approximately constant after the decrease on April 18. For higher values of L following the initial decrease, the flux increased with time in approximately

an exponential manner. The time constant for this increase is about 5 days at $3.3 \leq L < 3.4$ and decreases for larger L values to about 2 days at $3.7 \leq L < 3.8$.

The corresponding plots of the response of channel B during the same time interval are shown in Figures 4 and 5. It is seen that the changes in flux at this energy can be characterized by the same three regions as for channel A. However, the recovery time for $L \geq 3.3$ is seen to be longer and there is an indication that the flux did not return to the pre-strom value for $L \geq 3.0$.

Comparing Figure 1 to Figure 3, one sees that for $L \geq 3.6$ the flux of 0.52 Mev trapped protons changed in time in a manner quite similar to the time behavior of the D_{st} index. This fact is consistent with adiabatic deceleration and reacceleration of these protons in a manner similar to that observed by McIlwain [1966] for 40 to 110 Mev protons in the inner zone ($L \sim 2$). We do note, however, that the time behavior of 0.9 Mev protons is clearly nonadiabatic. The energy dependence of the deceleration-reacceleration process can be seen by examining the development of the energy spectrum.

Figures 6 and 7 show E_o versus time for the month of April for various L values with constant $|\vec{B}|$. E_o was approximately constant for April 1-17 for all L values above $L = 2.2$. The effect of the magnetic storm on the energy spectrum depends strongly

on L. For $L \leq 2.5$ there was no statistically significant change in E_o after the magnetic storm. For $2.5 \leq L \leq 2.8$, E_o increased gradually after the storm. For $L \geq 2.8$, the effect of the storm was a sharp reduction in E_o. For $2.8 \leq L \leq 3.3$, E_o was at a minimum value at 0902 UT on April 18 and then increased with time for about three days to values which were then constant. The final value of E_o for $2.8 \leq L < 2.9$ was higher then the pre-storm value, whereas for $L \geq 2.9$ the value of E_o after April 21 was below the pre-storm value.

B. Effect of the Sudden Commencement

The L dependence of the changes in fluxes associated with the magnetic storm are seen more clearly by showing the measured flux versus L for a constant $|\vec{B}|$ for individual satellite passes during the storm.

Figures 8 and 9 show the responses of the two channels plotted versus L for $0.18 \leq |\vec{B}| < 0.20$ gauss for passes before and after the sudden commencement. As indicated in the figures, these passes are at magnetic local times of 4.5 to 6 hours. The average for the period March 1-April 17 is also shown to indicate the pre-storm conditions. Of the four passes before the sudden commencement, only the one at 0753 UT shows fluxes which are at the pre-storm level for $L \sim 3.0$; all the others show reduced fluxes. The values of the spectral parameter E_o calculated from these passes are shown in Figure 10. The values of E_o are somewhat above the

pre-storm values for the three passes before 1141 UT. However on this pass the values are at the pre-storm average for $L \geq 3.3$. The first pass after the sudden commencement, at 1341 UT, shows reduced fluxes and increased values of E_o. Since this effect on E_o is much more pronounced in this pass than in either the one at 0559 UT or 0945 UT, it is probably attributable to the sudden commencement at ~ 1313 UT. Thus, it appears that the immediate effect of the sudden commencement was a general depression in the intensities and a hardening in the energy spectrum. The hardening in the spectrum persists until the onset of the main phase.

C. The Initial Phase

Cahill [1966] has shown that the magnetosphere is compressed during the initial phase of this magnetic storm. The effect of this compression on the trapped protons can be seen in Figures 8 and 9 for the pass at 0240 UT on April 18, at geographic local time of 4.0 hours. From the Hermanus magnetogram (located at 3.9 hours local time [Cahill, 1966]), the horizontal component of the magnetic field was near the maximum increase above the pre-storm level. Thus the satellite is still in the compressed magnetosphere for this pass. The fluxes measured by the two channels on this pass for $0.18 \leq |\vec{B}| < 0.20$ gauss are above the pre-storm levels for $2.6 \leq L \leq 3.2$. The values of E_o for this pass are shown versus L in Figure 10. These values are above the pre-storm values. The

effect of the positive initial phase of the magnetic storm is an enhancement of the proton fluxes at the energies measured here with no change from the sudden commencement spectrum.

D. Development of the Main Phase

The main phase field depression begins at most low-latitude ground stations between 0200 and 0300 UT on April 18. The responses of the two channels on the first few satellite passes after this decrease are shown in Figures 11 and 12. These passes are all at magnetic local times of 3.3 to 6.5 hours. The pass at 0514 UT shows reduced intensity for $L \leq 3.25$ for both channels. In addition, the intensity has increased at $L \geqslant 3.5$ for channel A. This increase occurs about one hour prior to a similar increase observed by Brown et.al. [1968] close to the equator with Explorer 26. Thus it appears that the initial increase at large L values may have commenced at small equatorial pitch angles. The next available data, the pass at 0902 UT, shows an increase for $L \leq 3.25$ and a decrease for $L \geq 3.25$. At 1055 UT the intensity is further increased for $L \leq 3.0$ and greatly reduced for $L \geq 3.0$, while on the next day the same general situation prevails.

An examination of the passes at 0514 and 0902 UT, together with Figure 13, reveals the following: (1) There was a loss of particles for $L \geqslant 3.2$ and a gain at $L \leqslant 3.2$ at both energies.

(2) For the latter region the spectrum has become softer, i.e., lower energy particles preferentially moved into this region. (3) For $L \geq 3.2$ the particle loss was the same for both low and high energies since the spectrum has maintained its post-sudden commencement form. These two passes may be compared with similar observations (Davis, private communication, 1971) on Explorer 26 at $E \geq 345$ kev at 40° equatorial pitch angle which show the particle loss down to L values of 2.8. This is an additional indication that particle increases commence at small equatorial pitch angles and progress towards 90°. We note here that particle loss, gain, and/or redistribution must have taken place during the polar substorm which lasted from ~ 0602 to ~ 0800 UT since no particle effects were observed following the onset of the storm main phase at ~ 0200 UT. Thus it appears that the polar substorm is imtimately associated with the mechanism(s) of proton acceleration and/or redistribution in this energy range.

E. The Recovery Phase

Figure 14 shows the responses for the two channels on four characteristic passes during the recovery phase. As can be seen in the figure, these passes have nearly the same $|\vec{B}|$ dependence and are at magnetic local times of 3.9 to 4.3 hours. The pass at 1609 UT on April 19 shows that both channels measured an intensity maximum at L = 2.85. The pass at 1125 UT on April 20 shows a

secondary peak in the distribution for channel A at $L \sim 3.5$. The pass at 1040 UT on April 21 shows that the secondary peak was still present and that the flux for $L \geq 3.5$ has increased, changing the shape of the profile. The pass at 1154 UT on April 22 shows that the flux had increased from the previous day for $L \geq 3.3$ and that the shape of the distribution had changed slightly. This pass on April 22 shows fluxes which are nearly equal to the post-storm average. Figure 14 shows that the data from channel B does not show the formation of a secondary maximum at 0.9 Mev.

F. The Steady-State Pre-Storm and Post-Storm Distributions

The net change in the proton distribution due to the magnetic storm is found by comparing the average flux for the pre-storm and post-storm periods. These two periods have been defined as March 1-April 17 and April 25-May 31. During each of these two periods the proton fluxes were approximately constant.

Figures 15 and 16 show the intensity versus L contours for $0.18 \leq |\vec{B}| < 0.20$ gauss for these two periods for the two channels. It is seen that the flux was unchanged for $L \leq 2.5$, increased for $2.5 \leq L \leq 3.0$, and reduced for $3.0 \leq L \leq 3.7$ for channel A and $L \geq 3.0$ for channel B. From these figures it is seen that the intensity maximum for the pre-storm distribution was at $L = 3.0 \pm 0.05$ for $0.18 \leq |\vec{B}| < 0.20$ gauss for both channels A and B. The post-storm maximum for the same $|\vec{B}|$ value was at $L = 2.8 \pm 0.05$ for both channels.

Figure 17 shows the L dependence of the measured spectral parameter E_o for these two periods for $0.18 \leq |\vec{B}| < 0.20$ gauss. It is seen that for $2.3 \leq L \leq 2.8$, E_o was increased after the storm period, and for $L > 3.0$ it was lower. In both distributions E_o was proportional to L^{-3} for higher L values. The region of this dependence for the pre-storm distribution was $3.4 \leq L \leq 4.4$, and for the post-storm distribution it was $2.6 \leq L \leq 4.4$. The dependence of E_o on L will be discussed in greater detail in a later section.

The over-all effect of the storm on the steady-state particle distribution may be seen by examining the $|\vec{B}|$,L intensity contours before and after the storm. Figure 18 shows constant intensity contours for channel A for the two periods March 1 to April 17 and April 25 to May 31. It is seen that: (1) There was no change in the distribution after the magnetic storm for the $|\vec{B}|$ values sampled here for $L \leq 2.5$. (2) For the pre-storm distribution the maximum intensity was observed at $L = 3$ at $|\vec{B}| = 0.19$ gauss for channel A. The maximum was at higher L values as $|\vec{B}|$ increased, being at $L = 3.2$ at $|\vec{B}| = 0.26$ gauss. For the post-storm distribution, the intensity maximum was at $L = 2.8$ for $0.16 \leq |\vec{B}| \leq 0.26$ gauss. (3) The secondary intensity peak evidently exists up to $|\vec{B}|$ values of at least 0.3 gauss and it moves to higher L values as $|\vec{B}|$ increases.

In general, there was a particle increase in a region bordered by $2.5 \leq L \leq 2.9$ and $0.18 \leq |\vec{B}| \leq 0.30$, and a decrease in the region bordered by $2.9 \leq L \leq 3.8$ and $0.18 \leq |\vec{B}| \leq 0.34$.

Figure 19 shows the corresponding constant intensity contours for channel B. From this figure it is seen that: (1) There was no change in the distribution after the magnetic storm for $L \leq 2.4$ for the $|\vec{B}|$ values sampled here. (2) As in the data of channel A, the intensity maximum occurred at lower L values for a given $|\vec{B}|$ value after the storm. The intensity maximum was at $L = 2.8$ for $0.16 \leq |\vec{B}| \leq 0.30$ gauss.

In general, there was a particle increase in the region bordered by $2.4 \leq L \leq 2.9$, $0.15 \leq |\vec{B}| \leq 0.30$ and a decrease in in the region bordered by $L \geq 2.9$ and $0.15 \leq |\vec{B}| \leq 0.30$.

The actual magnitude of the change in flux, defined by

$$\Delta j = j_{After} - j_{Before}$$

as a function of $|\vec{B}|$ for several L values for channel A can be seen in Figure 20. The over-all features are naturally the same as those found in the previous two figures. In the region where there was a general decrease, the net particle loss for $3.1 \leq L \leq 3.4$ increases as $|\vec{B}|$ decreases, i.e., the loss is larger at larger equatorial pitch angles. However the <u>fractional</u> loss at

each $|\vec{B}|$ value is approximately the same $\left(\frac{\Delta j}{j} \sim 0.3 \text{ to } 0.5\right)$, i.e., the same percentage of particles was lost at all pitch angles. For the L range $3.4 \leq L \leq 3.8$, there exists a peak in the Δj versus $|\vec{B}|$ contour which reflects the presence of the secondary peak noted in the previous four plots. The fractional loss, however, is approximately constant even in this range of L. Although one may gain the impression that Δj becomes zero or positive as one approaches the equator, the data of Söraas and Davis [1968] show that the same fractional decrease (~ 0.6) was observed for equatorial particles. It appears that in the range $3.0 \leq L \leq 3.7$ and for all pitch angles there was a loss of 0.52 Mev protons. Further, for $2.5 \leq L \leq 3$, there was an increase which was also present at all the pitch angles observed here and may have extended to the equator.

5. SUMMARY OF OBSERVATIONS

In the preceding sections we have presented data which show the redistribution of trapped protons following the April 17, 1965, magnetic storm. The most important features of the observations may be summarized as follows:

(a) There was a semi-permanent increase in the intensity of 0.52 and 0.90 Mev trapped protons at $L \leqslant 3.0$ and a similar decrease at $L \geqslant 3.0$.

(b) All changes were energy-dependent as reflected in the change of the energy parameter E_o.

(c) The immediate effect of the sudden commencement on trapped protons was a general depression in the intensities and a hardening of the energy spectrum.

(d) During the initial phase, particle intensities were enhanced although the spectrum remained the same.

(e) The most important effects on the proton population during the main phase were observed following the polar substorm, although some intensity increases for 0.52 Mev protons were observed at $L \geqslant 3.5$ about one hour before the substorm.

(f) During the recovery phase a secondary intensity peak developed for 0.52 Mev protons at $L \geq 3.5$. No such peak was observed for 0.9 Mev protons.

(g) The energy spectrum following the storm became harder at $L \leq 2.8$ and softer at $L \geq 2.8$, and the $E_o \sim L^{-3}$ dependence was thus extended over a wider range in L.

(h) It appears that the loss and/or gain of particles was fractionally the same for a given L at all equatorial pitch angles observed here.

6. DISCUSSION

A. Overall Effects

It is apparent from the observations that the over-all effect of the April 17, 1965, magnetic storm was a nonadiabatic change in the distribution of low-energy ($E \geq 0.52$ Mev) trapped protons in the radiation belt. In addition, the redistribution profile was not monotonic, i.e., there was an increase in particle fluxes below $L \sim 3$ and a decrease above the same value. Similar behavior of protons at $1.2 \leq E \leq 2.2$ Mev for this storm has been observed at small pitch angles by Bostrom et. al. [1970], although the effects at $E_p \geq 2.2$ Mev were not as pronounced. Bostrom et. al. [1970] also show the effects of the May, 1967 magnetic storm, where the behavior of low-energy protrons was qualitatively similar in that increases were observed down to $L \sim 2$. Thus it appears that following a magnetic storm loss and gain of protons is limited both in spatial extent and in energy, although the distribution may vary from event to event. Following Bostrom et. al. [1970], we suggest that this may indicate a resonance phenomenon in the magnetosphere.

This view is supported by the observations of Söraas and Davis [1968] at large ($> 40°$) equatorial pitch angles where they observed a decrease in the flux of $E > 0.513$ Mev protons at

$L \geq 3$, although they show an increase for energies $0.134 \leq E \leq 0.300$ Mev. It is not clear whether the increase at $E \geq 0.52$ Mev observed at high latitudes at $2.5 \leq L \leq 3$ was also present at the equator because Söraas and Davis [1968] present data at $L = 2.5$ and $L = 3.0$, but not in the 2.5 to 3.0 interval.

Differences are observed, however, in the recovery of intensities at the equator when compared to those at high latitude. Specifically, it can be seen from Figure 3 that at $L \geq 3.7$ the intensity attained its pre-storm level by the time D_{st} had approached zero. Söraas and Davis show that the intensity at $L = 3.5$ and $L = 4$ had not attained its pre-storm level for at least 50 days after the storm. We conclude from this comparison that replenishment of low-energy protons occurs much faster at high latitudes than at the equator for these L values. We recognize, however, that the rate of replenishment could be the same at all pitch angles and still appear as a slow recovery at the equator because of the much higher initial fluxes there. It appears that although the same percentage of particles was lost at all pitch angles (section 4F), the percentage rate of recovery is much higher at high latitudes than at the equator.

The data presented here at values $3.1 \leq L < 3.7$ show a qualitatively similar behavior to those obtained at the equator, in that the observed recovery at high latitudes is very long

(> 44 days). The data of McIlwain [1966] for 40 Mev protons also show a nonadiabatic decrease at $L \geq 2.6$ which lasted for at least 20 days.

B. Sudden Commencement and Initial Phase

It was shown in section 4B that fluxes were decreased and the spectrum became harder following the sudden commencement. Such a hardening of the spectrum is expected from the compression of the magnetosphere during the initial phase. However, the effect of the compression on the fluxes is not readily discernable because the degree of compression on a given field line is not accurately known. The calculation of the expected intensity changes at a given point in B,L space are complicated by two competing effects: (1) The fact that one may be sampling the intensity on a field line having a larger pre-event L value, and (2) that particles having an energy which is originally below the detector threshold have now become energized and are counted by the detector. Hence it is not clear whether at a given L value the intensity should increase or decrease, and by what amount. We note the fluxes did return to their pre-sudden commencement level as the initial phase developed.

C. Main Phase and Recovery Phase

As remarked in section 4, the effects on the particle distribution during the main phase occurred during and after the polar substorm. It can be seen from Figures 11 to 13 that large changes in the particle distribution took place well after (~ 1100 UT) the substorm had subsided (~ 0800 UT). In fact the particle gain at $L \leq 3.0$ and loss at $L \geq 3.0$ was more or less complete by 1100 UT and the intensity profile had not changed substantially 24 hours later.

The most striking feature of the recovery phase was the growth of a secondary intensity peak at $L \sim 3.5$ for 0.52 Mev protons, but not for 0.90 Mev ones. Davis (private communication, 1971) does not observe a similar peak at 0.513 Mev at the equator for at least seven days after the substorm. Figure 14 shows that the peak had already developed by April 20. We must then conclude that at this energy (0.52 Mev) there was injection of new particles at small equatorial pitch angles. It is possible that a similar number of particles was injected at all pitch angles, but that the fractional increase at large pitch angles was too small to be observed. It is not possible to identify the origin of these injected particles without full knowledge of the complete time history at all pitch angles and L values.

D. The Proton-Energy Spectrum

The steady-state energy spectrum before and after the storm may be understood in terms of bimodal diffusion as discussed by Theodoridis et. al. [1969]. Briefly, the model attempts to reproduce trapped particle intensity profiles by use of two competing diffusion processes, one of which conserves the first adiabatic invariant μ and the other the particle energy E. If the probability of constant μ diffusion is denoted by F_1 while that for constant E diffusion is denoted by F_2, Theodoridis et. al. obtain good agreement with observed proton profiles for F_2/F_1 ratios of 0.1 to 0.025. Further, by introducing enhanced μ diffusion over short periods of time ($\sim$ 1 day), the bimodal diffusion model is able to reproduce a secondary proton peak in the intensity-L profile which is qualitatively similar to the one actually observed for 0.52 Mev protons following the geomagnetic storm.

The most remarkable accomplishment of the model, however, appears to be the accurate prediction of the dependence of E_o on L. Theodoridis et. al. show that the steady-state profile of E_o versus L can be generally separated into three different regions: (1) For $L \leq 3$, $E_o \propto L^{-\delta}$ where δ is much less than 3, and could be as small as 1. (2) For $3 \leq L \leq 4.5$, the value of $\delta \sim 3$. (3) For $L \geq 4.5$ to 5, E_o is more or less independent of L. This behavior is accurately similar to the pre-storm distribution observed in

Figure 17, and is obtained for $F_2/F_1 \sim 0.1$. Following strong geomagnetic activity the bimodal diffusion model predicts a wider L range of applicability for the $E_o \sim L^{-3}$ relation as is observed in our post-storm distribution also shown in Figure 17. Unfortunately, the observations do not extend beyond $L \sim 4.5$ so that the range over which E_o is independent of L cannot be checked. We do note, however, that this 'knee' in the E_o versus L profile was also observed at the equator for $L \geq 4$ by Krimigis and Armstrong [1966] and Armstrong and Krimigis [1968]. It appears that an adjustment of the constants used by Theodoridis et. al. [1969] may result in a detailed reproduction of the experimental results in the bimodal diffusion approximation.

It is apparent from the above that the qualitative behavior of the spectrum before and after the April 17, 1965, storm can be satisfactorily accounted for by the bimodal diffusion model. Constant μ diffusion alone would not be able to account for the observations.

As a general comment, we note that the low-altitude high-latitude observations such as those presented in this paper should prove extremely useful in obtaining information on the effectiveness of pitch angle diffusion in populating small equatorial pitch angles in the manner discussed by Haerendel [1970].

ACKNOWLEDGMENTS

We thank Dr. J. A. Van Allen for his continued help and encouragement during this study. We are grateful for the efforts of many University of Iowa and Langley Research Center personnel, too numerous to mention by name, for their efforts in making the Injun 4 satellite a success.

This research was supported in part by the National Aeronautics and Space Administration under grant NGL 16-001-002 and the Office of Naval Research Contract N000-14-68-A-0196-0003.

REFERENCES

Akasofu, S. I., Electrodynamics of the magnetosphere: geomagnetic storms, Space Science Reviews, 6, 21-143, 1966.

Armstrong, T. P., and S. M. Krimigis, Observations of protons in the magnetosphere and magnetotail with Explorer 33, J. Geophys. Res., 73, 143-152, 1968.

Bame, S. J., J. P. Conner, H. H. Hill, and F. E. Holly, Protons in the outer Van Allen belt, (abstract) J. Geophys. Res., 67, 1628, 1962.

Bostrom, C. O., D. S. Beall, and J. C. Armstrong, Time history of the inner radiation zone, October 1963 to December 1968, J. Geophys. Res., 75, 1246-1255, 1970.

Brown, W. L., L. J. Cahill, L. R. Davis, C. E. McIlwain, and C. S. Roberts, Acceleration of trapped particles during a magnetic storm on April 18, 1965, J. Geophys. Res., 73, 153-161, 1968.

Burns, A. L., Effects of the 17 April 1965 magnetic storm on trapped protons, Master's thesis, University of Iowa, Iowa City, Iowa, 52240, 1968.

Cahill, L. J., Jr., Inflation of the inner magnetosphere during a magnetic storm, J. Geophys. Res., 71, 4505-4519, 1966.

Davis, L. R., and J. M. Williamson, Outer Zone Protons in Radiation Trapped in the Earth's Magnetic Field, edited by B. M. McCormac, pp. 215-229, D. Reidel, Dordrecht, Holland, 1966.

Haerendel, G., On the balance between radial and pitch angle diffusion, in Particles and Fields in the Magnetosphere, edited by B. M. McCormac, pp. 416-428, D. Reidel, Dordrecht, Holland, 1970.

Krimigis, S. M., and T. P. Armstrong, Observations of protons in the magnetosphere with Mariner 4, J. Geophys. Res., 71, 4641-4650, 1966.

Krimigis, S. M., and J. A. Van Allen, Geomagnetically trapped alpha particles, J. Geophys. Res., 72, 5779-5797, 1967.

Lincoln, J. V., Geomagnetic and Solar Data, J. Geophys. Res., 71, 1477-1479, 1965.

McIlwain, C. E., Ring current effects on trapped particles, J. Geophys. Res., 70, 3623-3628, 1966.

Meng, C. I., and S. I. Akasofu, The geomagnetic storm of April 17-18, 1965, J. Geophys. Res., 72, 4905-4916, 1967.

Nakada, M. P., and G. D. Mead, Diffusion of protons in the outer radiation belt, J. Geophys. Res., 70, 4777-4791, 1965.

Sŏraas, F., and L. R. Davis, Temporal variations of the 100 kev to 1700 kev trapped protons observed on satellite Explorer 26 during first half of 1965, Goddard Space Flight Center preprint no. X-612-68-328, August, 1968.

Theodoridis, G. C., F. R. Paolini, and S. Frankenthal, Acceleration of trapped electrons and protons through bimodal diffusion in the earth's radiation belts, J. Geophys. Res., 74, 1238-1253, 1969.

Tverskoy, V. A., Dynamics of the radiation belts of the earth: 2, Geomagnetism and Aeronomy, 351-366, 1964.

Williams, D. J., Trapped protons ≥ 100 kev and possible sources, in Particles and Fields in the Magnetosphere, edited by B. M. McCormac, pp. 396-409, D. Reidel, Dordrecht, Holland, 1970.

FIGURE CAPTIONS

Figure 1. The three hour K_p index (IAGA Commission IV, Geophysikalisches Institut, University of Gottingen) and the D_{st} index (Sugiura and Hendricks, Goddard Space Flight Center, Greenbelt, Maryland) for the month of April 1965.

Figure 2. The response of channel A vs time for the month of April 1965 with $0.18 \leq |\vec{B}| < 0.20$ gauss for the region $2.2 \leq L \leq 3.0$.

Figure 3. Same as Figure 2 for $3.0 \leq L \leq 3.8$.

Figure 4. The response of channel B vs time for the month of April 1965 for $0.16 \leq |\vec{B}| < 0.18$ gauss and $0.18 \leq |\vec{B}| < 0.20$ gauss for the region $2.2 \leq L \leq 3.0$.

Figure 5. Same as Figure 4 for $0.18 \leq |\vec{B}| < 0.20$ gauss and $3.0 \leq L \leq 3.8$.

Figure 6. The spectral parameter E_o vs time for April 1965 with constant $|\vec{B}|$ and L. The data are for $0.16 \leq |\vec{B}| < 0.18$ gauss and $0.18 \leq |\vec{B}| < 0.20$ gauss for $2.2 \leq L \leq 2.8$.

Figure 7. Same as Figure 6 with $0.18 \leq |\vec{B}| < 0.20$ gauss and $0.20 \leq |\vec{B}| < 0.22$ for $2.8 \leq L \leq 4.1$.

Figure 8. The response of channel A vs L for satellite passes on April 17 and 18. The data are for $0.18 \leq |\vec{B}| < 0.20$ gauss. As indicated, the magnetic local times for these passes are from 3.3 to 6.8 hours.

Figure 9. Same as Figure 8 for channel B.

Figure 10. The spectral parameter E_o vs L for satellite passes on April 17 and 18, calculated from the data shown in Figures 8 and 9. The solid line drawn for each pass shows the pre-storm average for the period March 1 to April 17, 1965, for $0.18 \leq |\vec{B}| < 0.20$ gauss.

Figure 11. The response of channel A vs L for satellite passes on April 18 and 19 for $0.18 \leq |\vec{B}| < 0.20$ gauss. The data are for magnetic local times of 4.6 to 6.5 hours. The solid line for each pass is the average for March 1 to April 17 for the same $|\vec{B}|$ value. Note the large change in the profile from 0900 to 1100 UT, well after the end of the substorm (~ 0800 UT).

Figure 12. Same as Figure 11 for channel B.

Figure 13. The spectral parameter E_o vs L for the four passes on April 18 and 19 shown in Figures 11 and 12. Data is for $0.18 \leq |\vec{B}| < 0.20$ gauss and $0.20 \leq |\vec{B}| < 0.22$ gauss. The solid line through the data is the average for $0.18 \leq |\vec{B}| < 0.20$ gauss for the period March 1 to April 17. The dashed line is the average for the same $|\vec{B}|$ value for the period April 25 to May 31, 1965.

Figure 14. Response of channels A and B vs L for four satellite passes on April 19 to April 22, 1965. As indicated, the passes all have nearly the same $|\vec{B}|$ dependence. The magnetic local times for these passes are from 3.9 to 4.3 hours.

Figure 15. Intensity vs L profiles for channel A for the two periods March 1 to April 17 and April 25 to May 31, 1965, for $0.18 \leq |\vec{B}| < 0.20$ gauss.

Figure 16. Same as Figure 15 for channel B.

Figure 17. The spectral parameter E_o vs L for the two periods March 1 to April 17 and April 25 to May 31, 1965, for $0.18 \leq |\vec{B}| < 0.20$ gauss. Both scales are logarithmic and both solid lines have slopes of -3.

Figure 18. Constant intensity contours for channel A for the two periods March 1 to April 17 and April 25 to May 31, 1965.

Figure 19. Same as Figure 18 for channel B.

Figure 20. The net change in flux, Δj, vs $|\vec{B}|$ for constant values of L in the interval $2.4 \leq L \leq 3.7$. Δj is defined as $\Delta j = (j_{After} - j_{Before})$ where After and Before refer to the periods April 25 to May 31 and March 1 to April 17, respectively. Note that the fractional change $\Delta j/j$ is roughly constant at all B values.

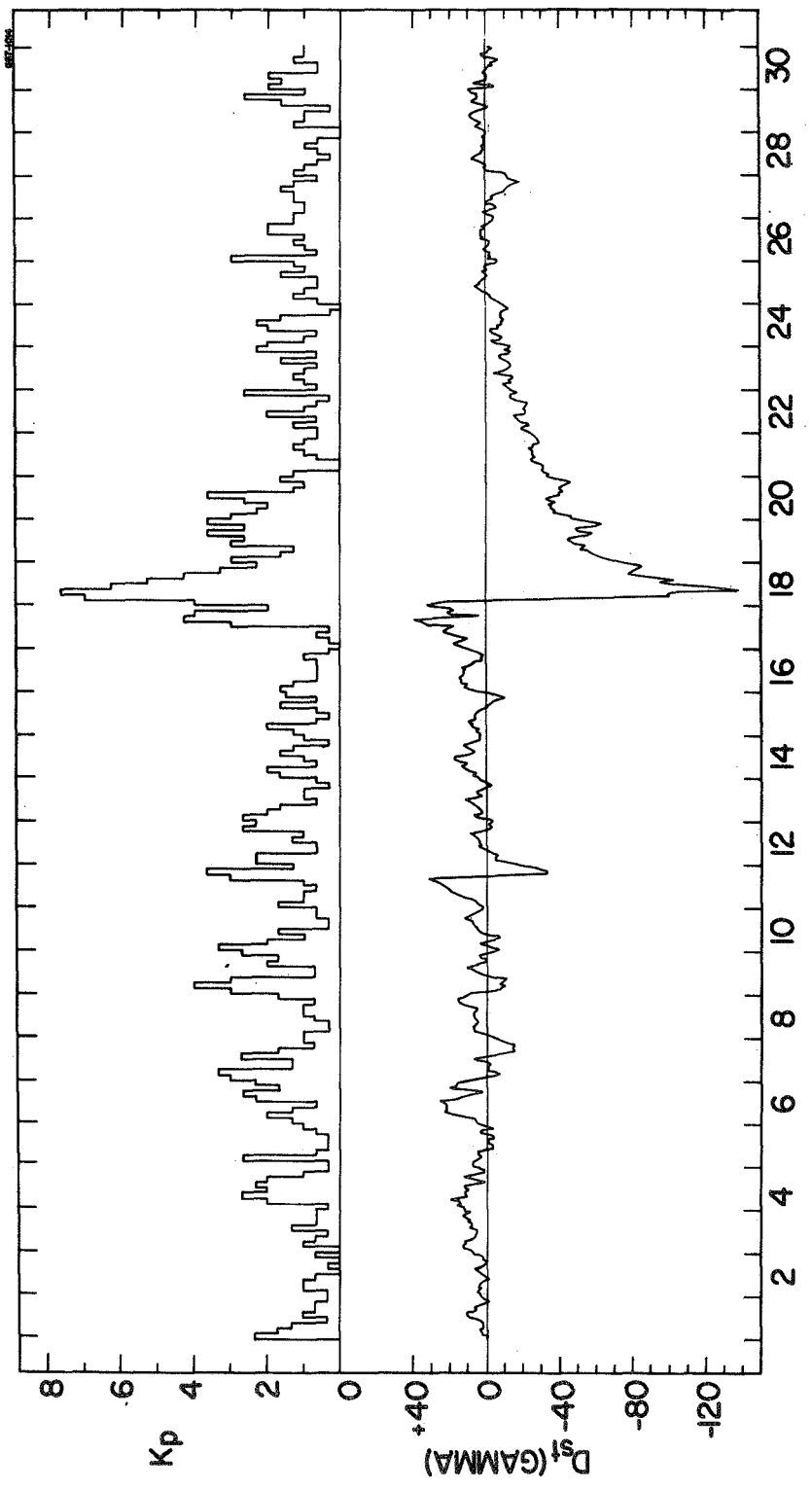
Kp
8
6
4
2
0
D_{st} (GAMMA)
+40
0
-40
-80
-120
2
4
6
8
10
12
14
16
18
20
22
24
26
28
30
DAY, APRIL, 1965

Figure 1.

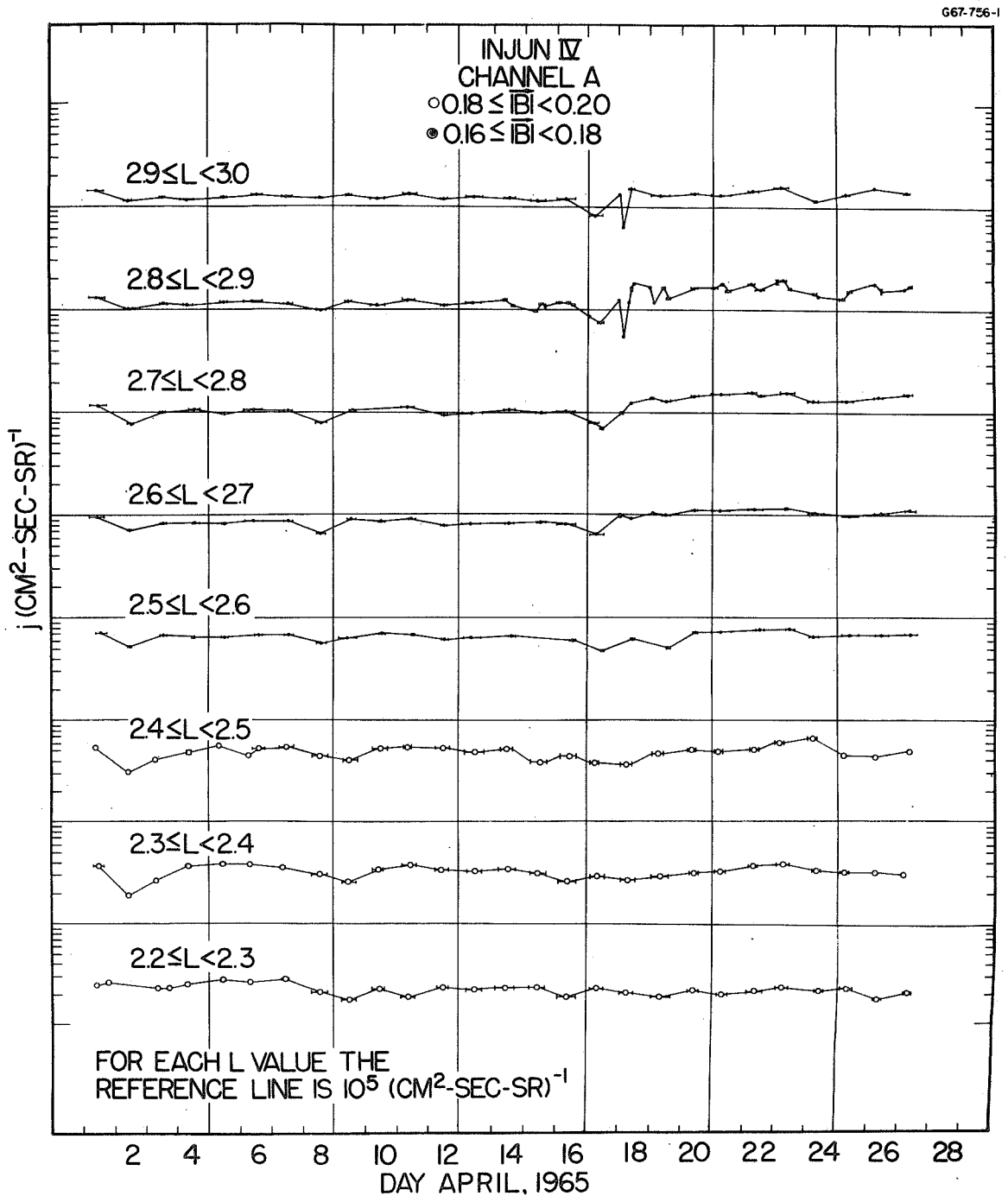
G67-756-1
INJUN IV
CHANNEL A
○0.18 ≤ |B| < 0.20
◉0.16 ≤ |B| < 0.18
2.9≤L<3.0
2.8≤L<2.9
2.7≤L<2.8
2.6≤L<2.7
2.5≤L<2.6
2.4≤L<2.5
2.3≤L<2.4
2.2≤L<2.3
FOR EACH L VALUE THE
REFERENCE LINE IS 10⁵ (CM²-SEC-SR)⁻¹
j (CM²-SEC-SR)⁻¹
2 4 6 8 10 12 14 16 18 20 22 24 26 28
DAY APRIL, 1965

Figure 2.

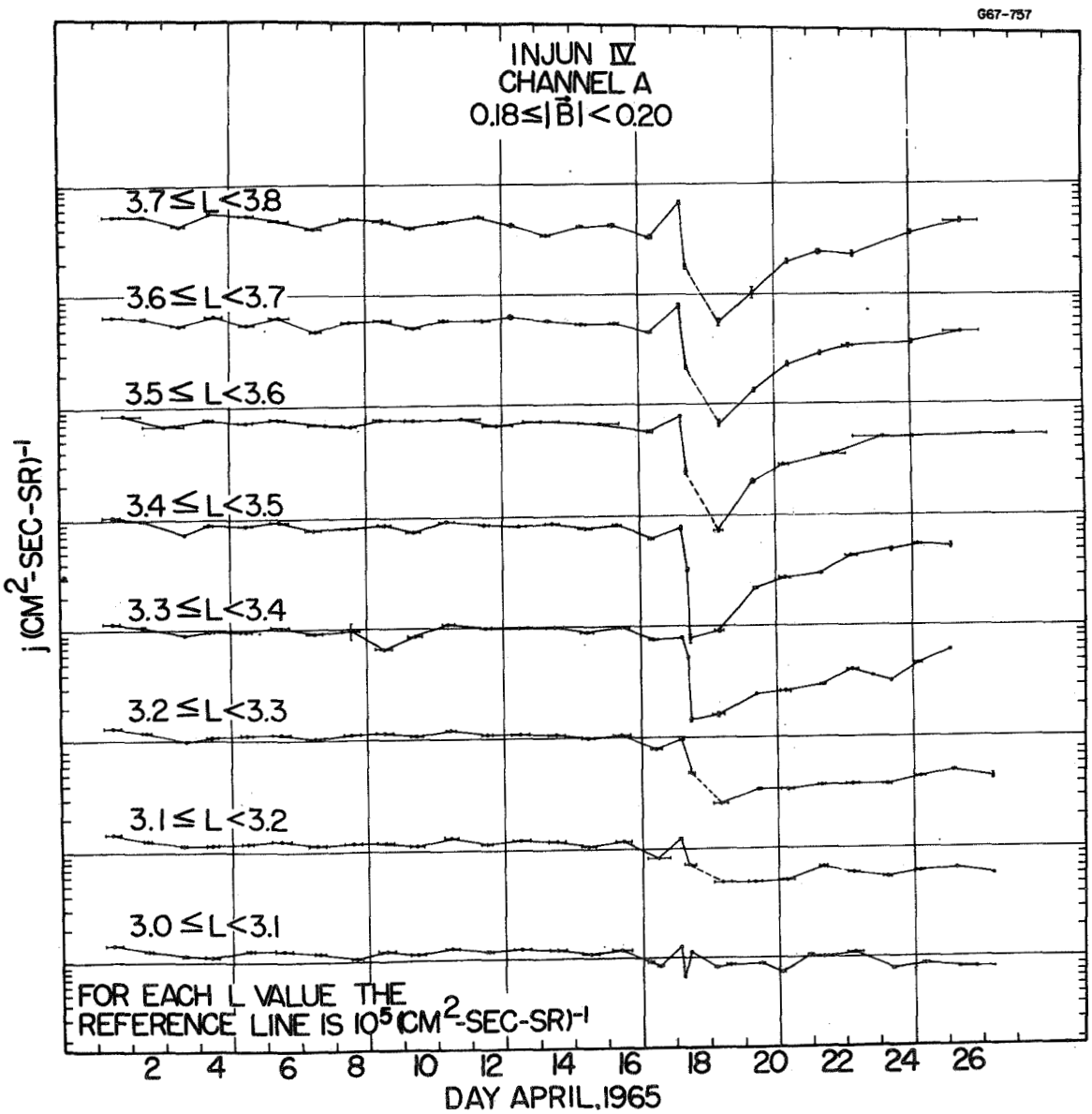
G67-757
INJUN IV
CHANNEL A
0.18≤|B|<0.20
3.7≤L<3.8
3.6≤L<3.7
3.5≤L<3.6
3.4≤L<3.5
3.3≤L<3.4
3.2≤L<3.3
3.1≤L<3.2
3.0≤L<3.1
j (CM2-SEC-SR)-1
FOR EACH L VALUE THE
REFERENCE LINE IS 10^5 (CM2-SEC-SR)-1
2 4 6 8 10 12 14 16 18 20 22 24 26
DAY APRIL, 1965

Figure 3.

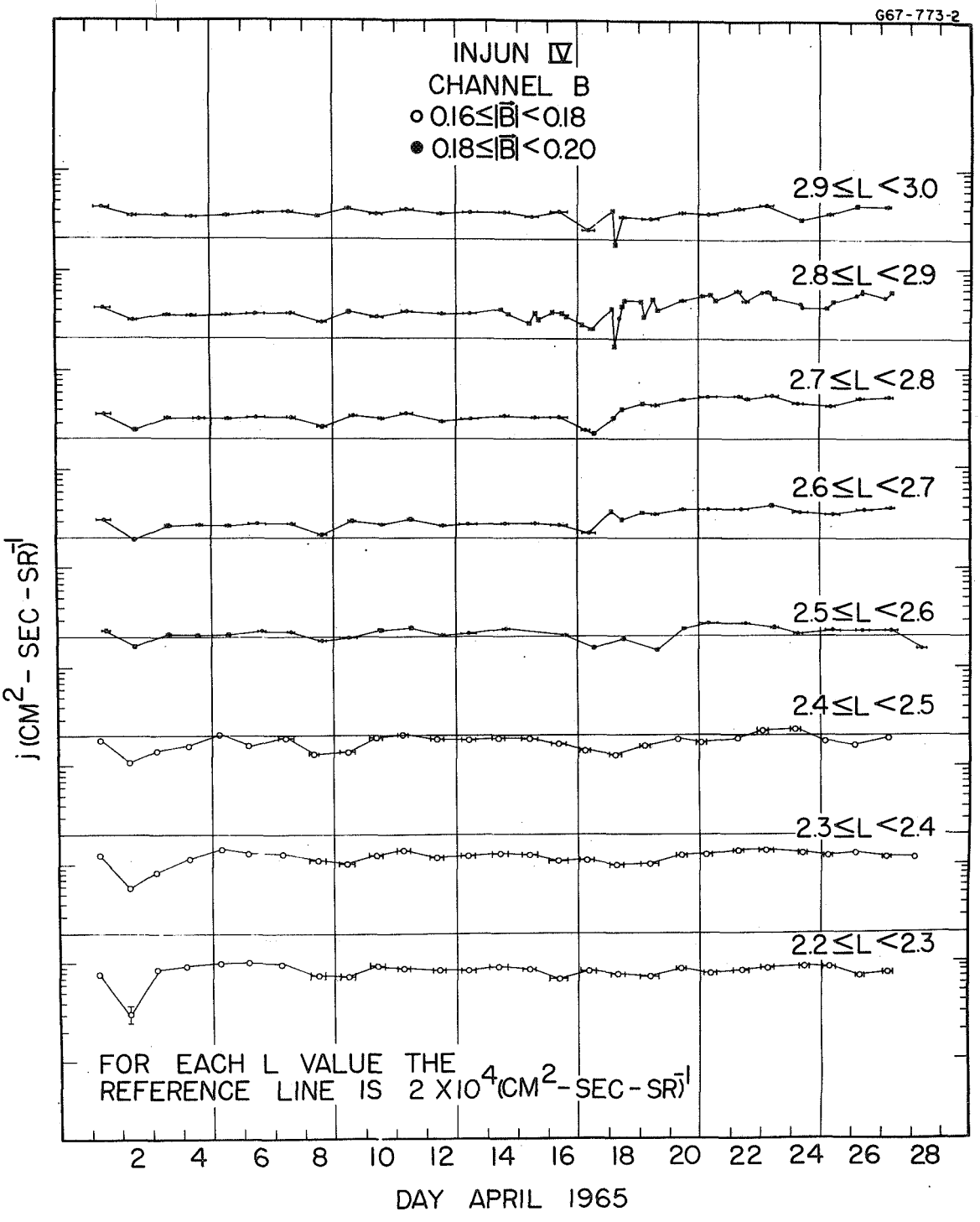
G67-773-2
INJUN IV
CHANNEL B
o 0.16≤|B|<0.18
● 0.18≤|B|<0.20
2.9≤L<3.0
2.8≤L<2.9
2.7≤L<2.8
2.6≤L<2.7
2.5≤L<2.6
2.4≤L<2.5
2.3≤L<2.4
2.2≤L<2.3
FOR EACH L VALUE THE REFERENCE LINE IS 2 X10^4 (CM^2 - SEC - SR)^-1
j (CM^2 - SEC - SR)^-1
2 4 6 8 10 12 14 16 18 20 22 24 26 28
DAY APRIL 1965

Figure 4.

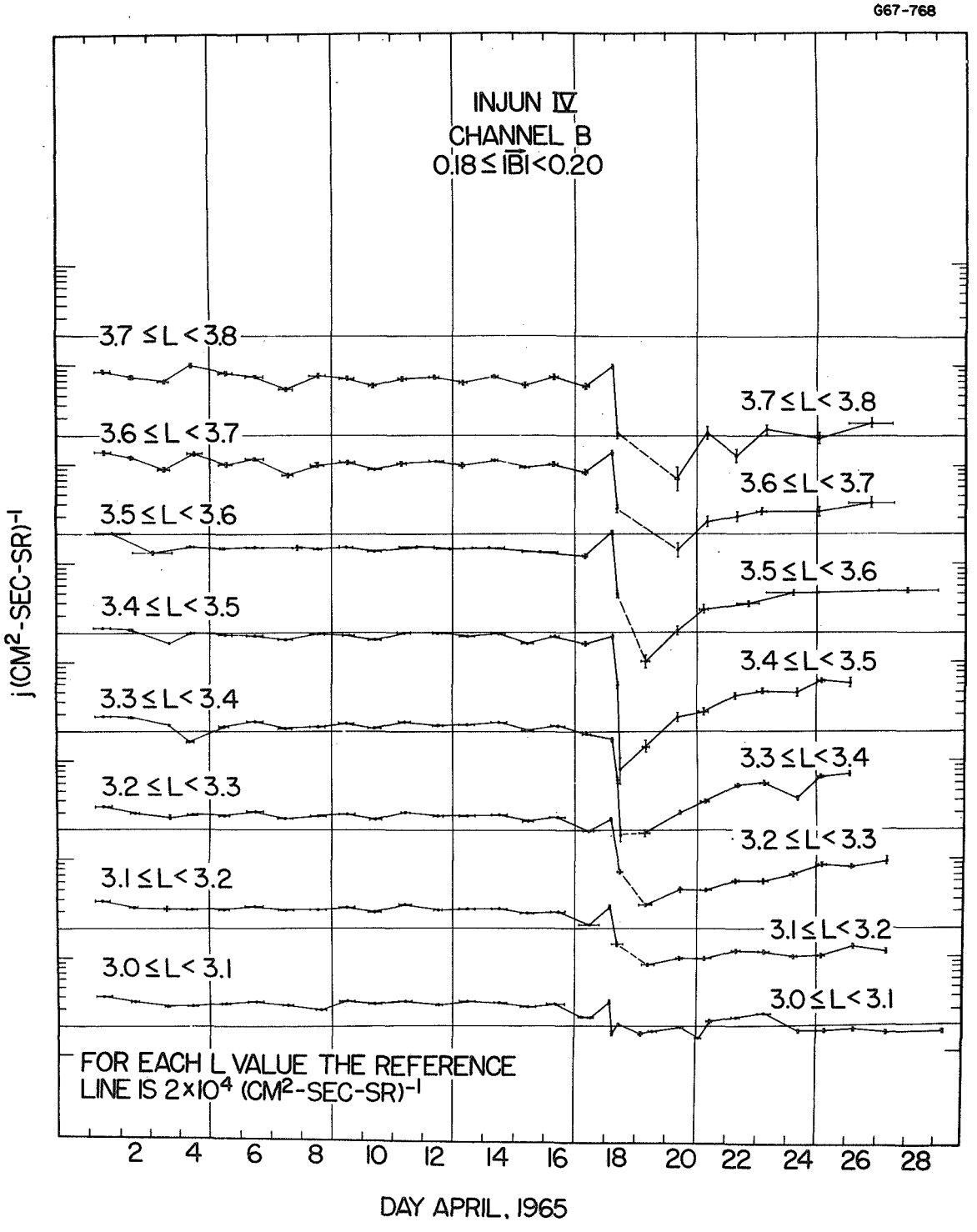
G67-768
INJUN IV
CHANNEL B
0.18 ≤ |B| < 0.20
3.7 ≤ L < 3.8
3.6 ≤ L < 3.7
3.5 ≤ L < 3.6
3.4 ≤ L < 3.5
3.3 ≤ L < 3.4
3.2 ≤ L < 3.3
3.1 ≤ L < 3.2
3.0 ≤ L < 3.1
FOR EACH L VALUE THE REFERENCE LINE IS 2×10⁴ (CM²-SEC-SR)⁻¹
j (CM²-SEC-SR)⁻¹
2 4 6 8 10 12 14 16 18 20 22 24 26 28
DAY APRIL, 1965

Figure 5.

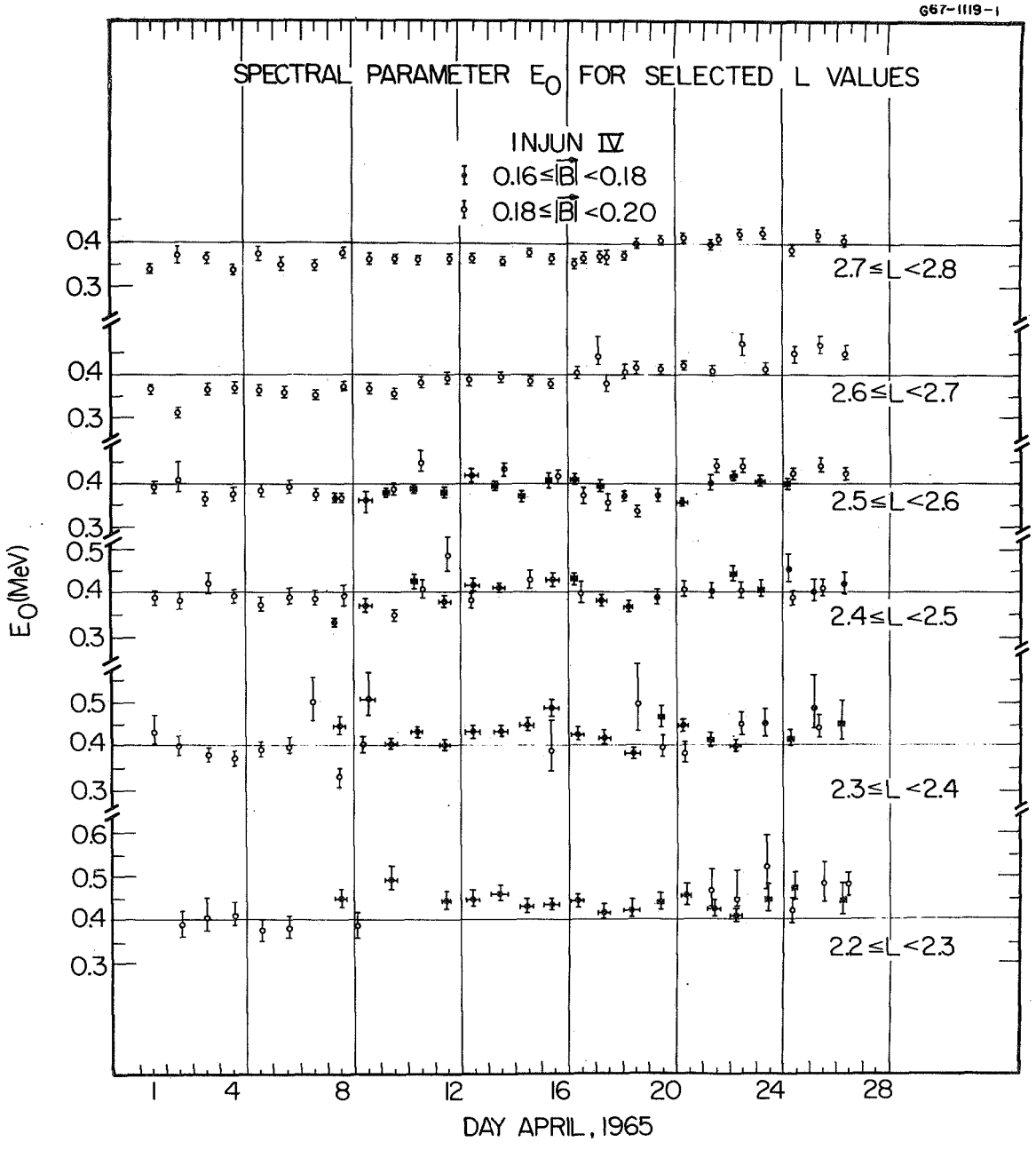
G67-1119-1
SPECTRAL PARAMETER E_0 FOR SELECTED L VALUES
INJUN IV
$0.16 \leq |\vec{B}| < 0.18$
$0.18 \leq |\vec{B}| < 0.20$
$2.7 \leq L < 2.8$
$2.6 \leq L < 2.7$
$2.5 \leq L < 2.6$
$2.4 \leq L < 2.5$
$2.3 \leq L < 2.4$
$2.2 \leq L < 2.3$
E_0(MeV)
0.6
0.5
0.4
0.3
1
4
8
12
16
20
24
28
DAY APRIL, 1965

Figure 6.

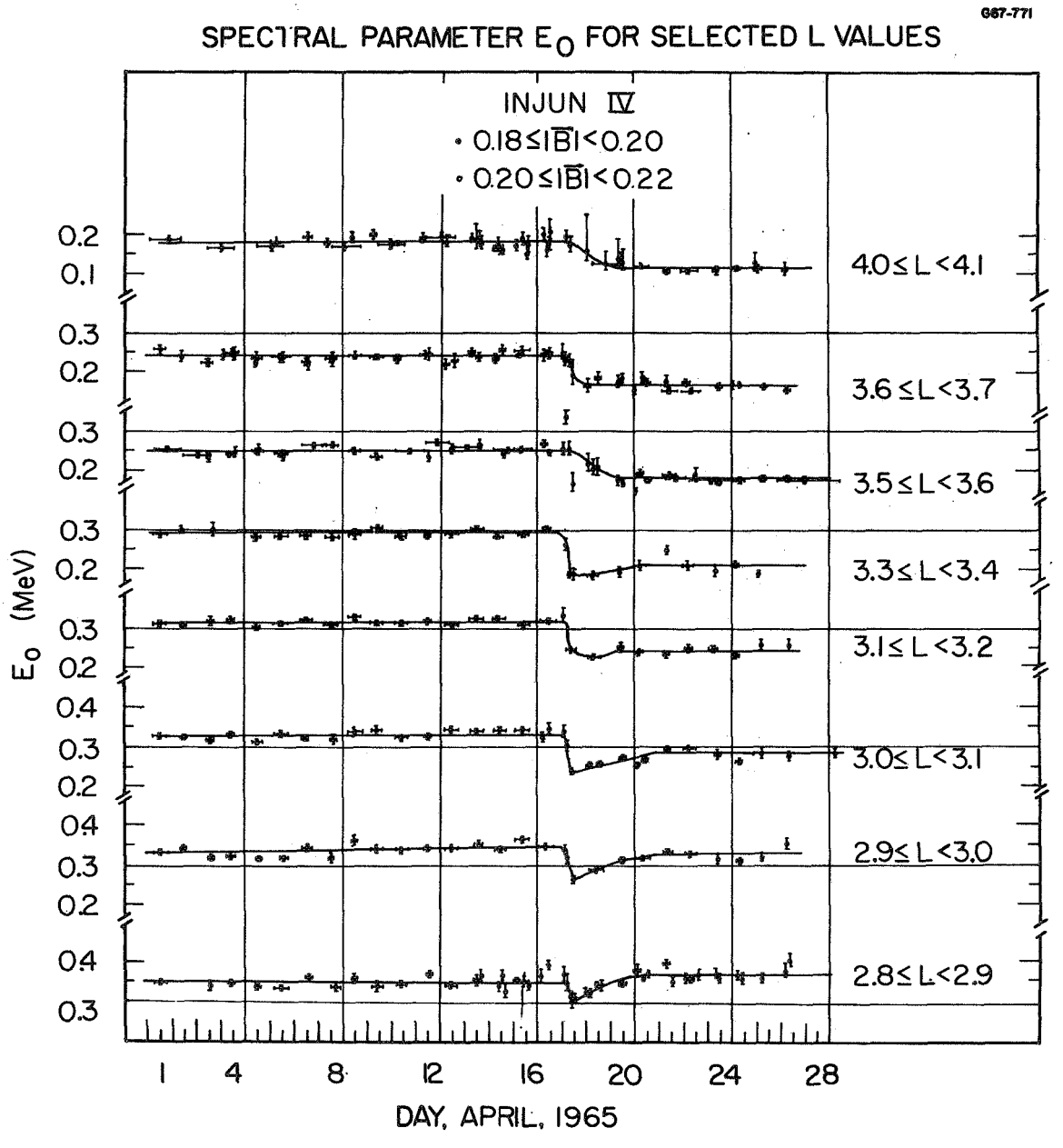
G67-771
SPECTRAL PARAMETER E_0 FOR SELECTED L VALUES
INJUN IV
• 0.18≤|B̄|<0.20
• 0.20≤|B̄|<0.22
4.0≤L<4.1
3.6≤L<3.7
3.5≤L<3.6
3.3≤L<3.4
3.1≤L<3.2
3.0≤L<3.1
2.9≤L<3.0
2.8≤L<2.9
E_0 (MeV)
0.2
0.1
0.3
0.2
0.3
0.2
0.3
0.2
0.3
0.2
0.4
0.3
0.2
0.4
0.3
0.2
0.4
0.3
1
4
8
12
16
20
24
28
DAY, APRIL, 1965

Figure 7.

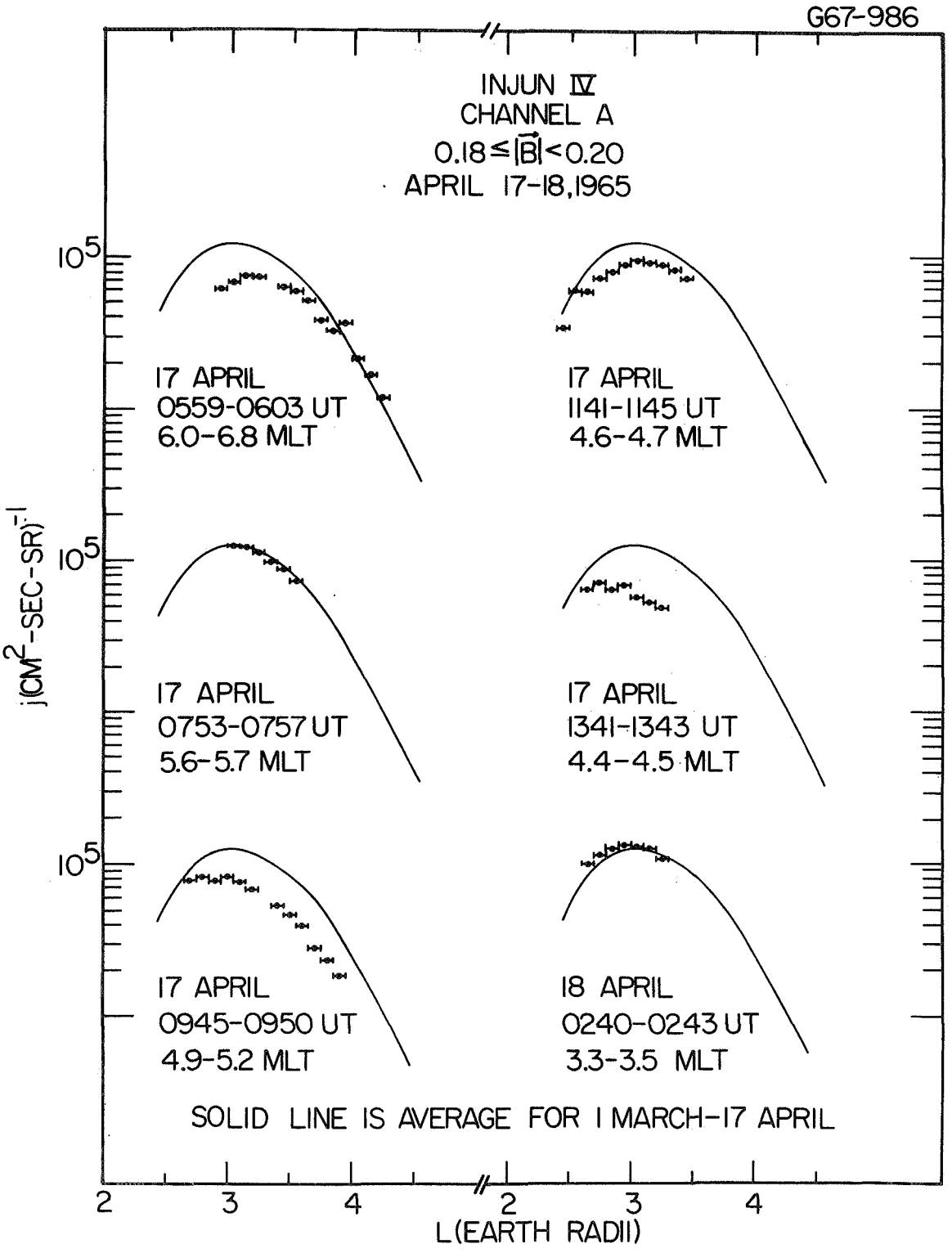
G67-986
INJUN IV
CHANNEL A
0.18≤|B|<0.20
APRIL 17-18,1965
17 APRIL
0559-0603 UT
6.0-6.8 MLT
17 APRIL
1141-1145 UT
4.6-4.7 MLT
17 APRIL
0753-0757 UT
5.6-5.7 MLT
17 APRIL
1341-1343 UT
4.4-4.5 MLT
17 APRIL
0945-0950 UT
4.9-5.2 MLT
18 APRIL
0240-0243 UT
3.3-3.5 MLT
SOLID LINE IS AVERAGE FOR 1 MARCH-17 APRIL
10^5
10^5
10^5
j(CM^2-SEC-SR)^-1
2
3
4
2
3
4
L(EARTH RADII)

Figure 8.

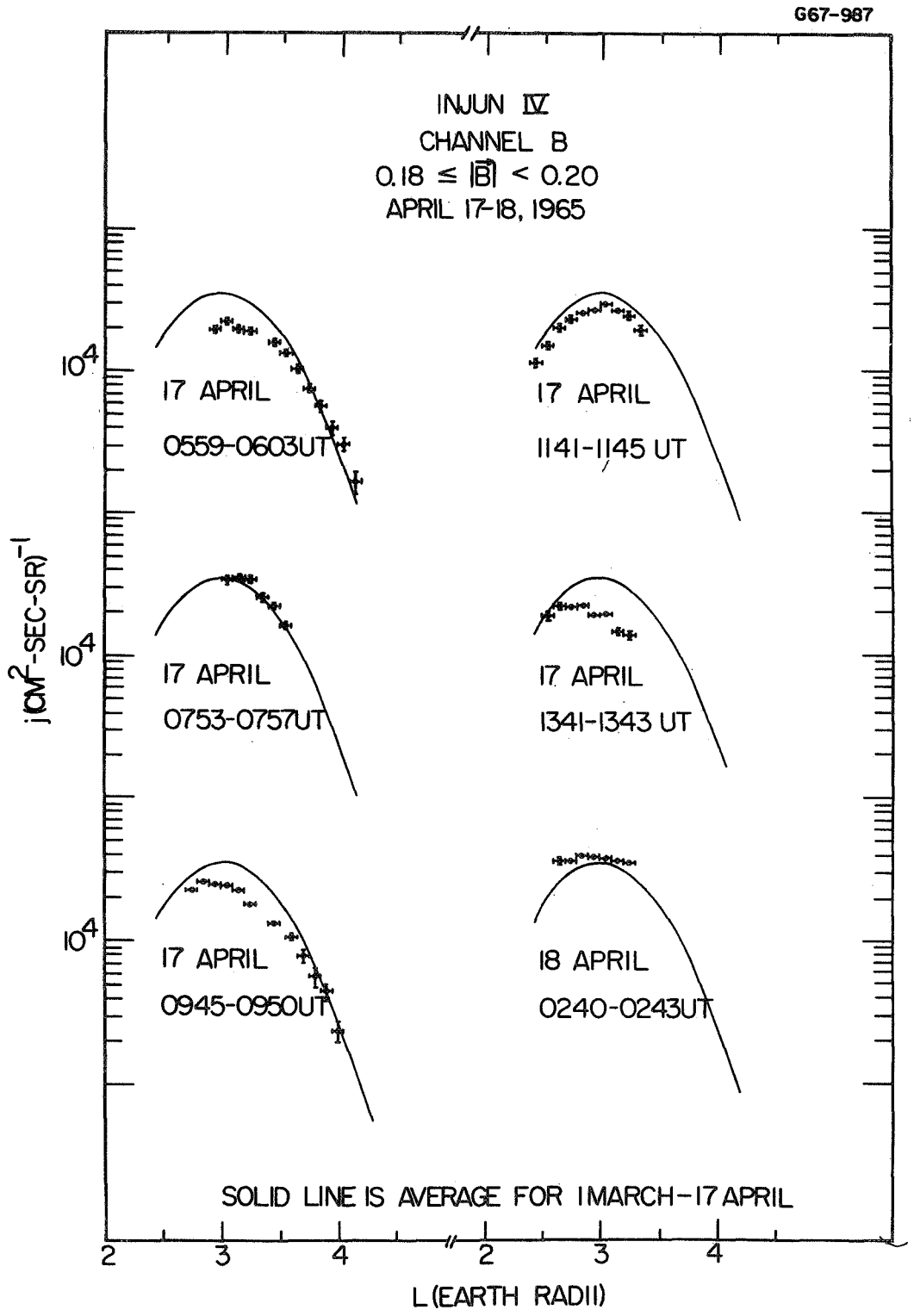
G67-987
INJUN IV
CHANNEL B
0.18 ≤ |B| < 0.20
APRIL 17-18, 1965
17 APRIL
0559-0603UT
17 APRIL
1141-1145 UT
17 APRIL
0753-0757UT
17 APRIL
1341-1343 UT
17 APRIL
0945-0950UT
18 APRIL
0240-0243UT
10^4
10^4
10^4
j(CM^2-SEC-SR)^-1
SOLID LINE IS AVERAGE FOR 1 MARCH-17 APRIL
2
3
4
2
3
4
L(EARTH RADII)

Figure 9.

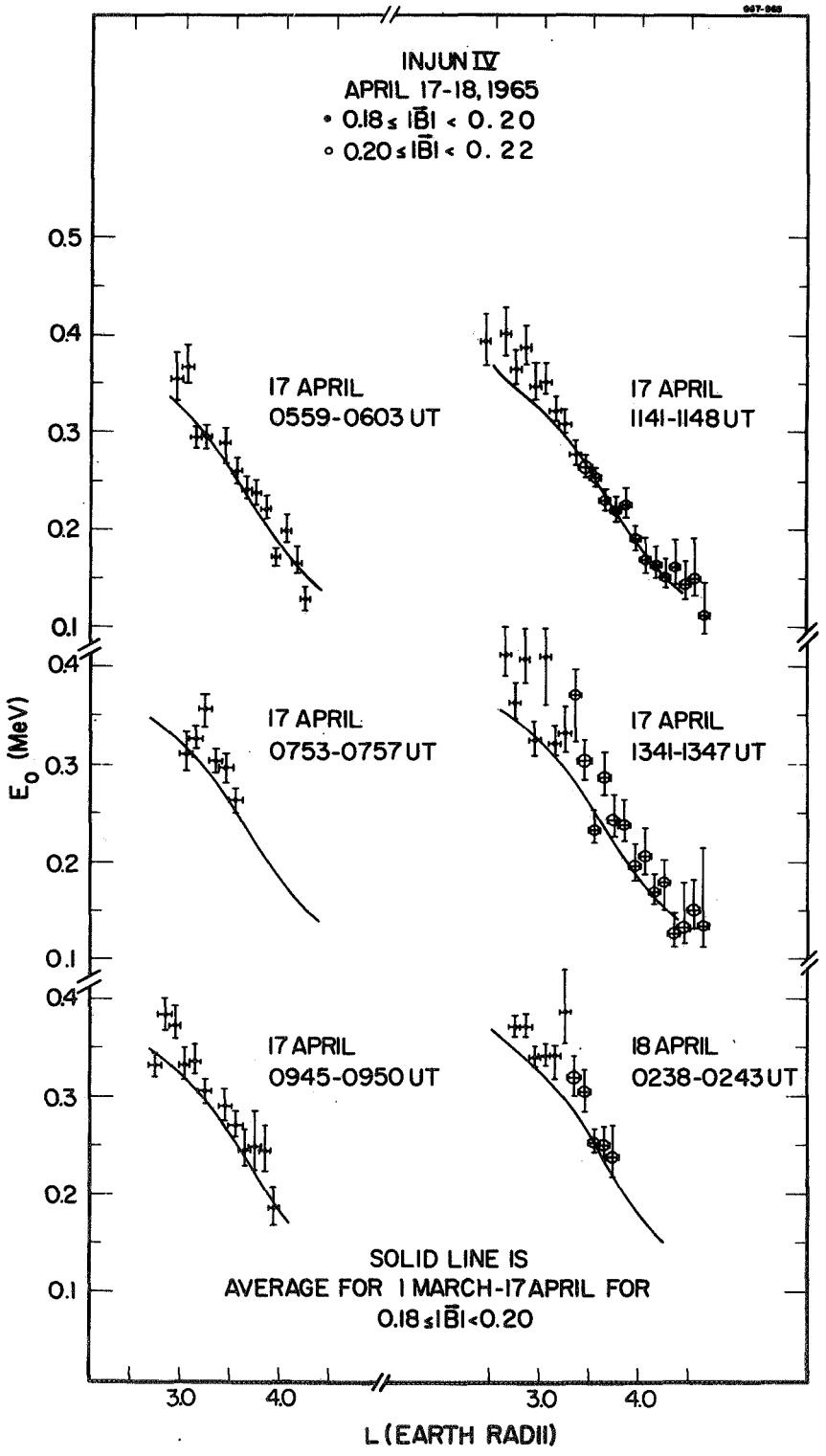
INJUN IV
APRIL 17-18, 1965
• 0.18 ≤ |B| < 0.20
∘ 0.20 ≤ |B| < 0.22
17 APRIL
0559-0603 UT
17 APRIL
1141-1148 UT
17 APRIL
0753-0757 UT
17 APRIL
1341-1347 UT
17 APRIL
0945-0950 UT
18 APRIL
0238-0243 UT
SOLID LINE IS
AVERAGE FOR 1 MARCH-17 APRIL FOR
0.18 ≤ |B| < 0.20
E0 (MeV)
0.5
0.4
0.3
0.2
0.1
3.0
4.0
L (EARTH RADII)

Figure 10.

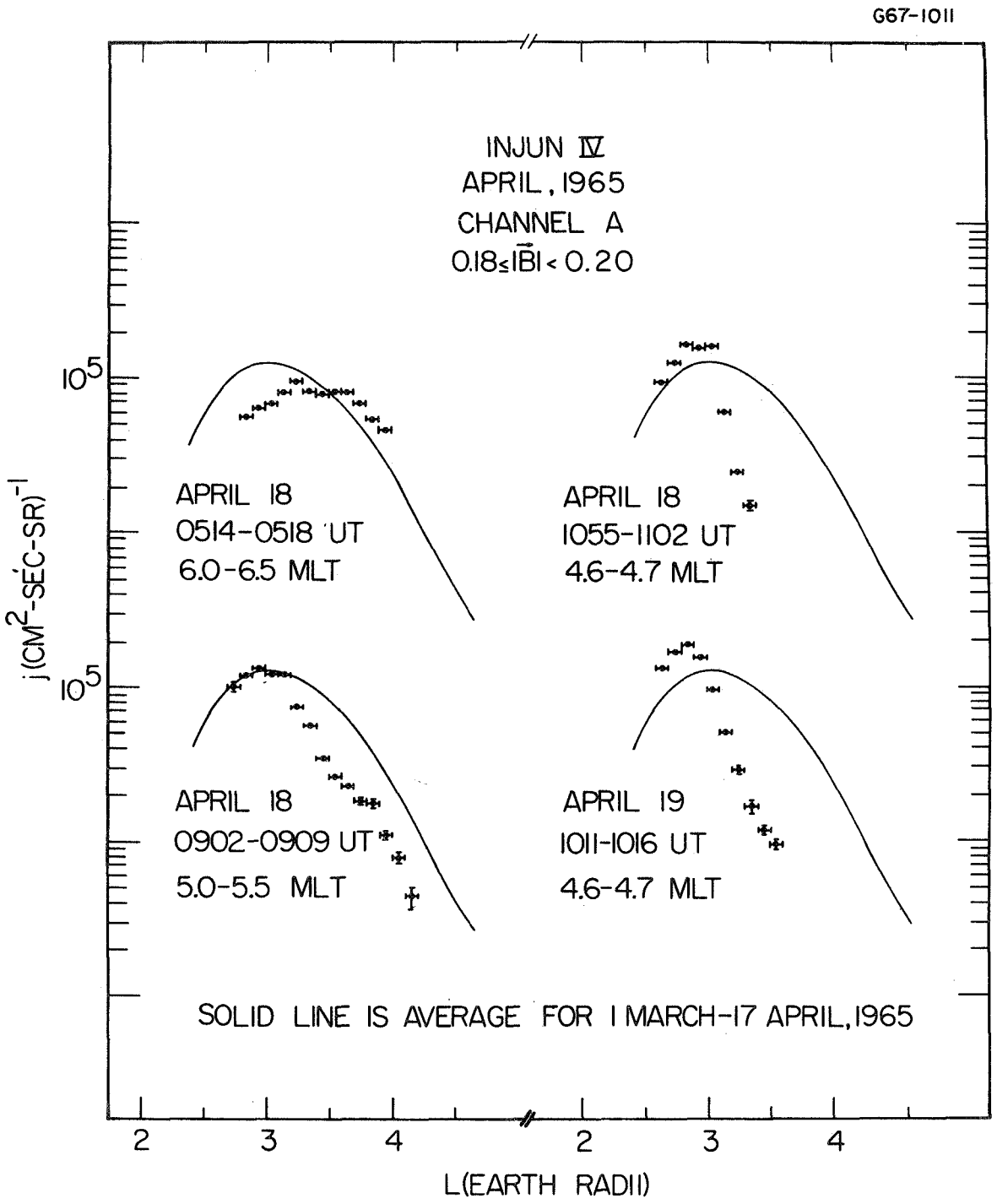
G67-1011
INJUN IV
APRIL, 1965
CHANNEL A
0.18≤|B|<0.20
APRIL 18
0514-0518 UT
6.0-6.5 MLT
APRIL 18
1055-1102 UT
4.6-4.7 MLT
APRIL 18
0902-0909 UT
5.0-5.5 MLT
APRIL 19
1011-1016 UT
4.6-4.7 MLT
SOLID LINE IS AVERAGE FOR 1 MARCH-17 APRIL, 1965
j(CM²-SEC-SR)⁻¹
10⁵
10⁵
2
3
4
2
3
4
L(EARTH RADII)

Figure 11.

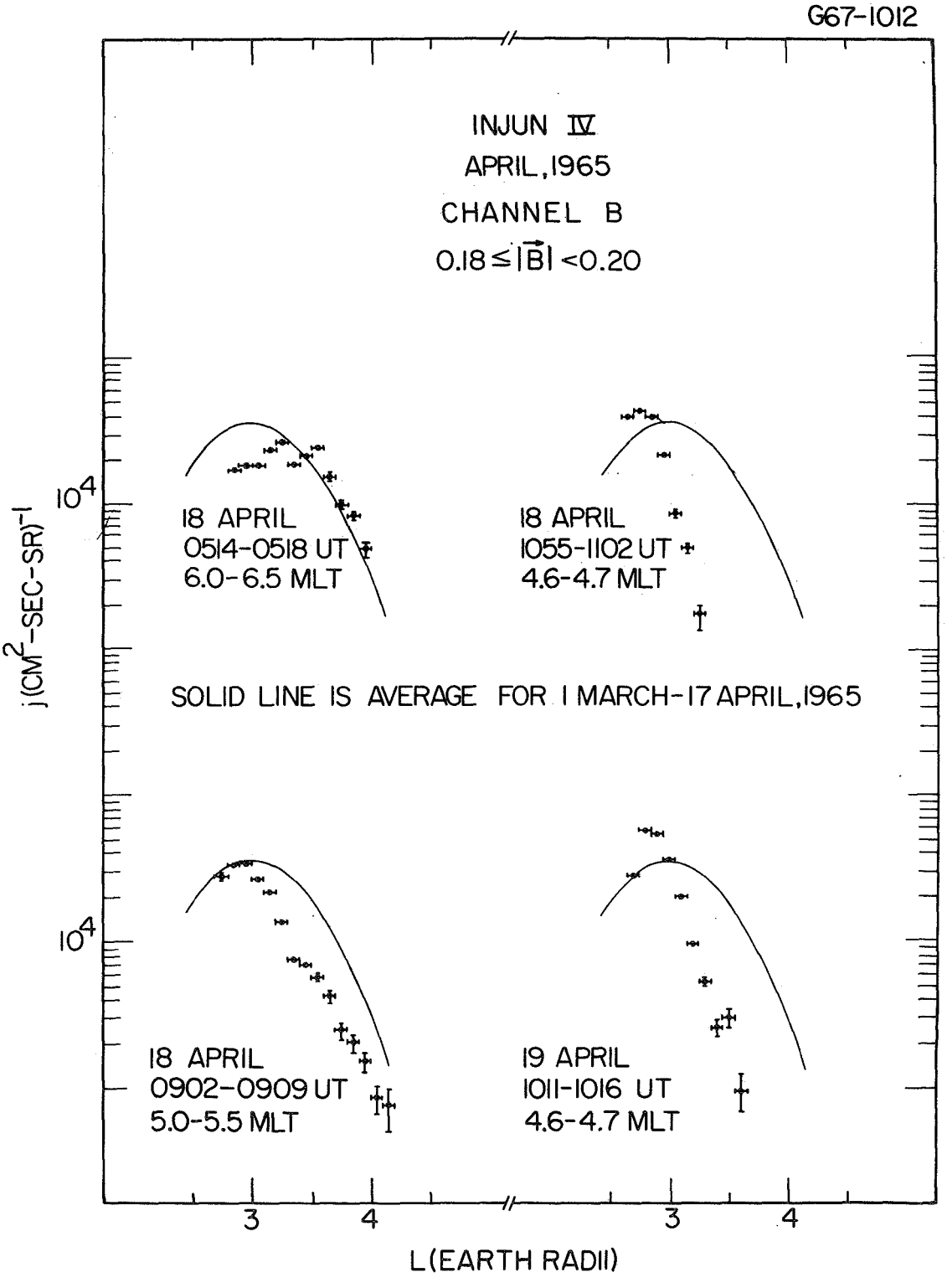
G67-1012
INJUN IV
APRIL, 1965
CHANNEL B
0.18 ≤ |B| < 0.20
18 APRIL
0514-0518 UT
6.0-6.5 MLT
18 APRIL
1055-1102 UT
4.6-4.7 MLT
SOLID LINE IS AVERAGE FOR 1 MARCH-17 APRIL, 1965
18 APRIL
0902-0909 UT
5.0-5.5 MLT
19 APRIL
1011-1016 UT
4.6-4.7 MLT
j(CM²-SEC-SR)⁻¹
10⁴
10⁴
3
4
3
4
L(EARTH RADII)

Figure 12.

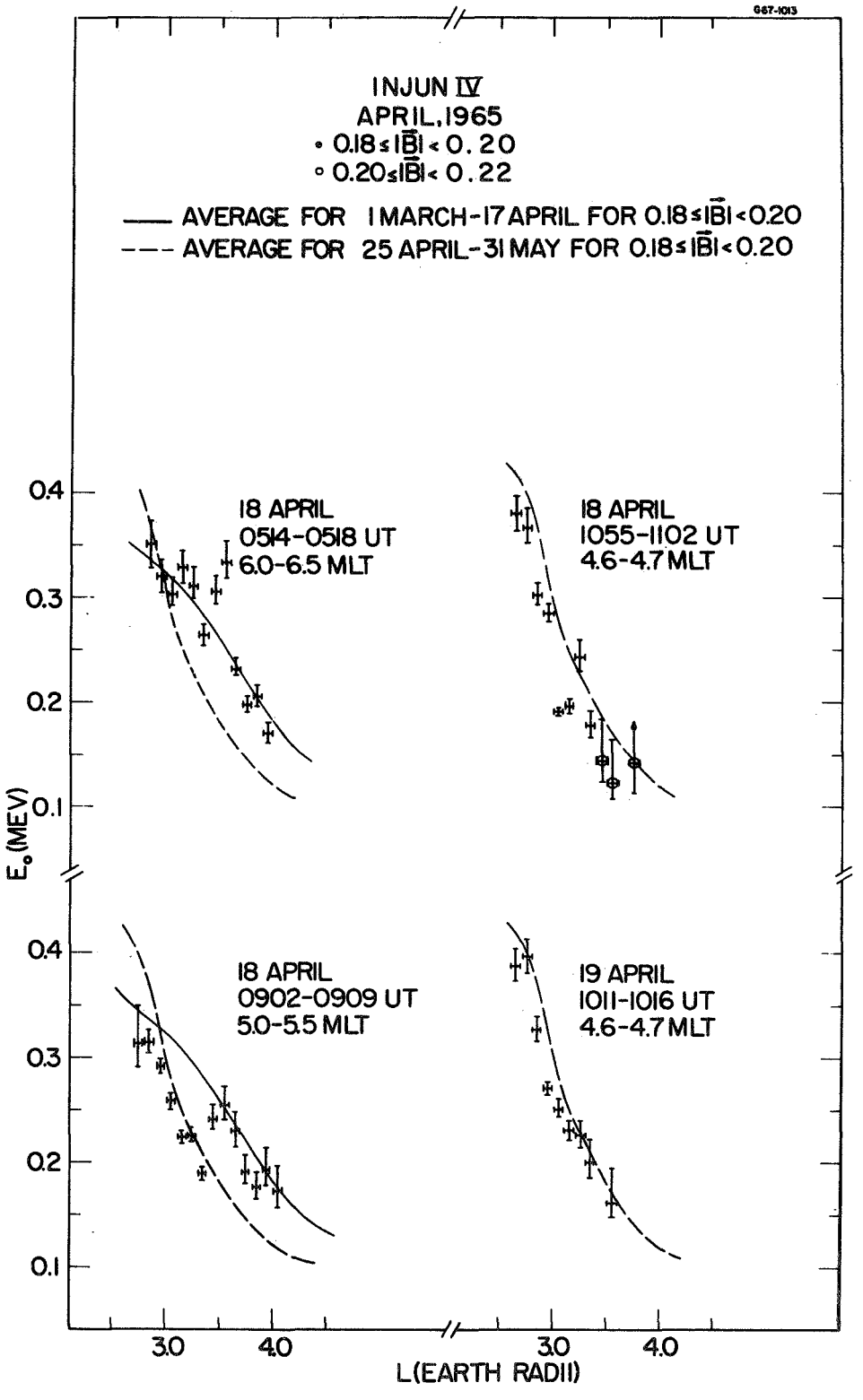
667-1013
INJUN IV
APRIL, 1965
• 0.18 ≤ |B| < 0.20
∘ 0.20 ≤ |B| < 0.22
—— AVERAGE FOR 1 MARCH-17 APRIL FOR 0.18 ≤ |B| < 0.20
--- AVERAGE FOR 25 APRIL-31 MAY FOR 0.18 ≤ |B| < 0.20
18 APRIL
0514-0518 UT
6.0-6.5 MLT
18 APRIL
1055-1102 UT
4.6-4.7 MLT
18 APRIL
0902-0909 UT
5.0-5.5 MLT
19 APRIL
1011-1016 UT
4.6-4.7 MLT
E₀ (MEV)
0.4
0.3
0.2
0.1
3.0
4.0
L(EARTH RADII)

Figure 13.

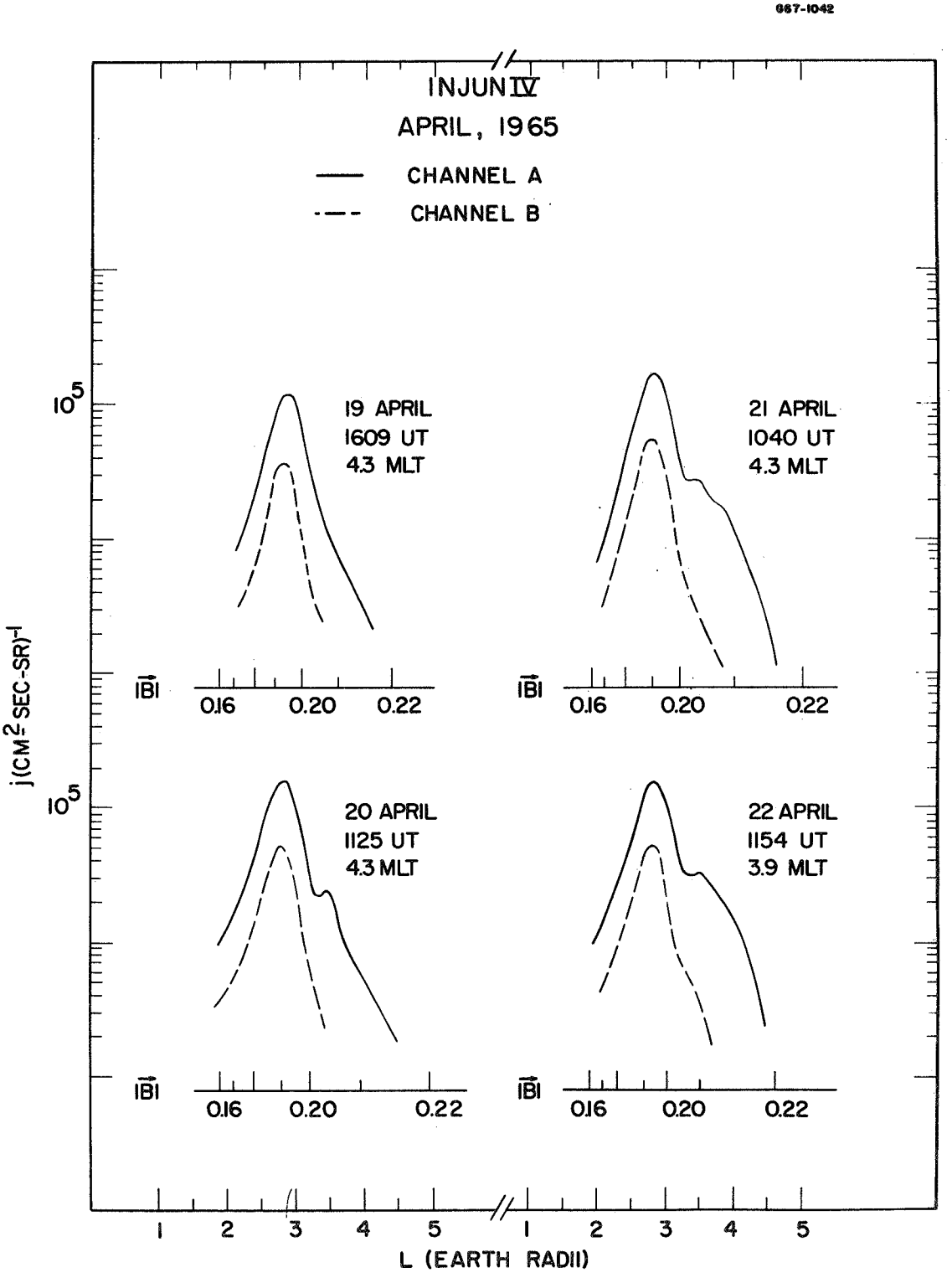
667-1042
INJUN IV
APRIL, 1965
CHANNEL A
CHANNEL B
19 APRIL
1609 UT
4.3 MLT
21 APRIL
1040 UT
4.3 MLT
20 APRIL
1125 UT
4.3 MLT
22 APRIL
1154 UT
3.9 MLT
|B|
0.16
0.20
0.22
10^5
j(CM^2 SEC-SR)$^{-1}$
1
2
3
4
5
L (EARTH RADII)

Figure 14.

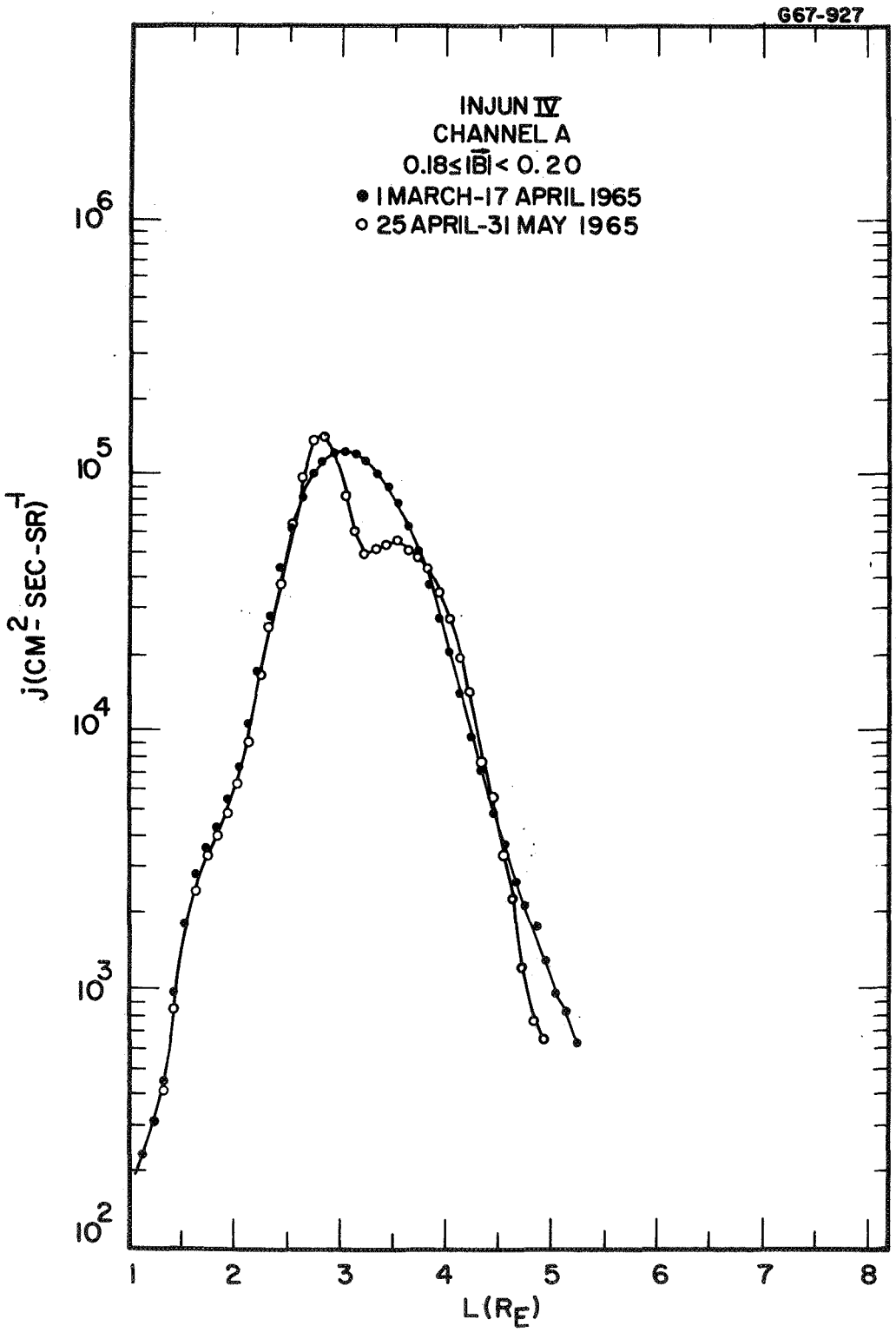
G67-927
INJUN IV
CHANNEL A
0.18≤|B|< 0.20
• 1 MARCH-17 APRIL 1965
○ 25 APRIL-31 MAY 1965
J(CM-2 SEC-SR)-1
10^6
10^5
10^4
10^3
10^2
1
2
3
4
5
6
7
8
L(RE)

Figure 15.

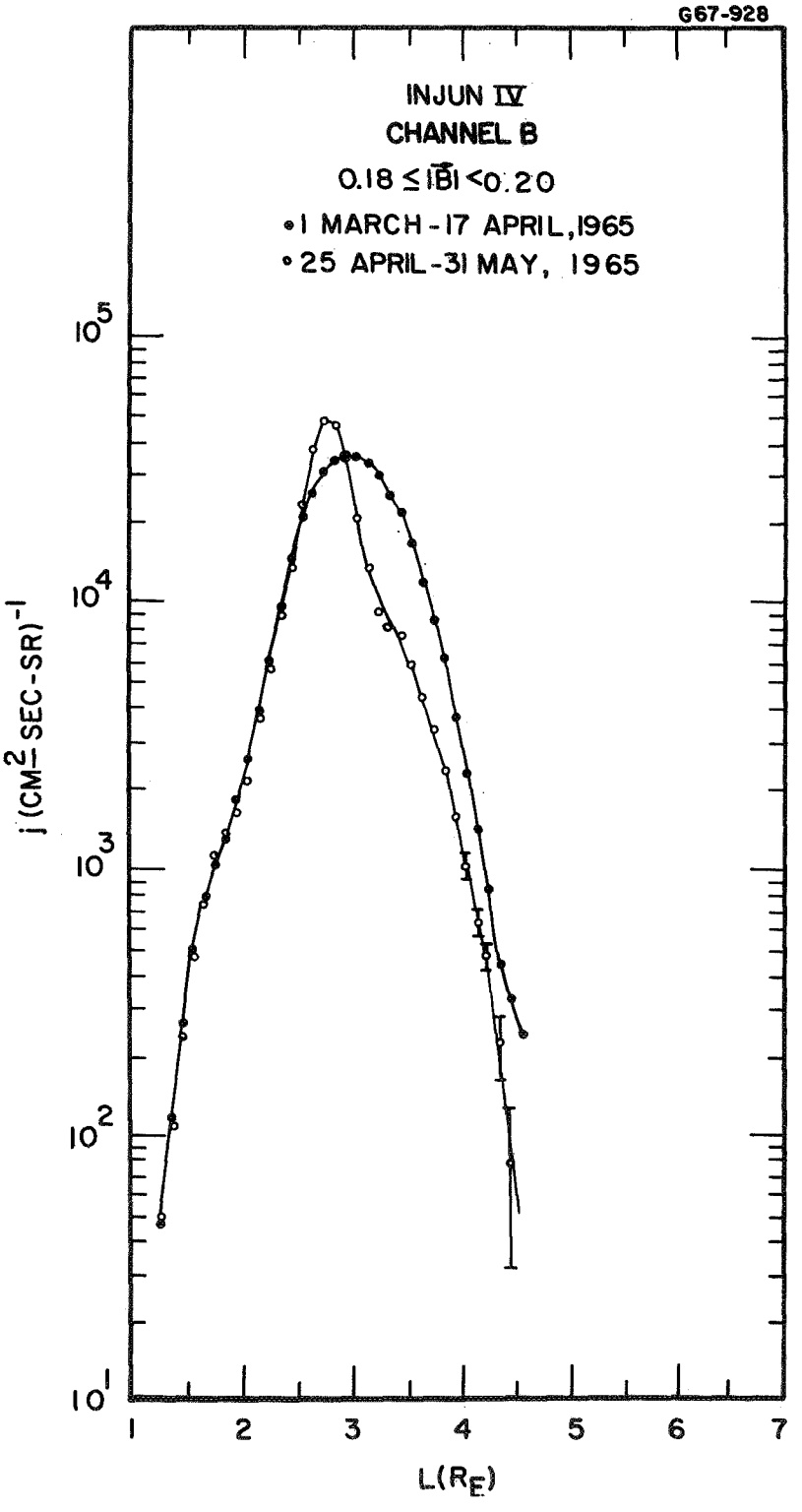
G67-928
INJUN IV
CHANNEL B
0.18 ≤ |B| < 0.20
• 1 MARCH - 17 APRIL, 1965
• 25 APRIL - 31 MAY, 1965
j (CM⁻² SEC-SR)⁻¹
10⁵
10⁴
10³
10²
10¹
1
2
3
4
5
6
7
L(R_E)

Figure 16.

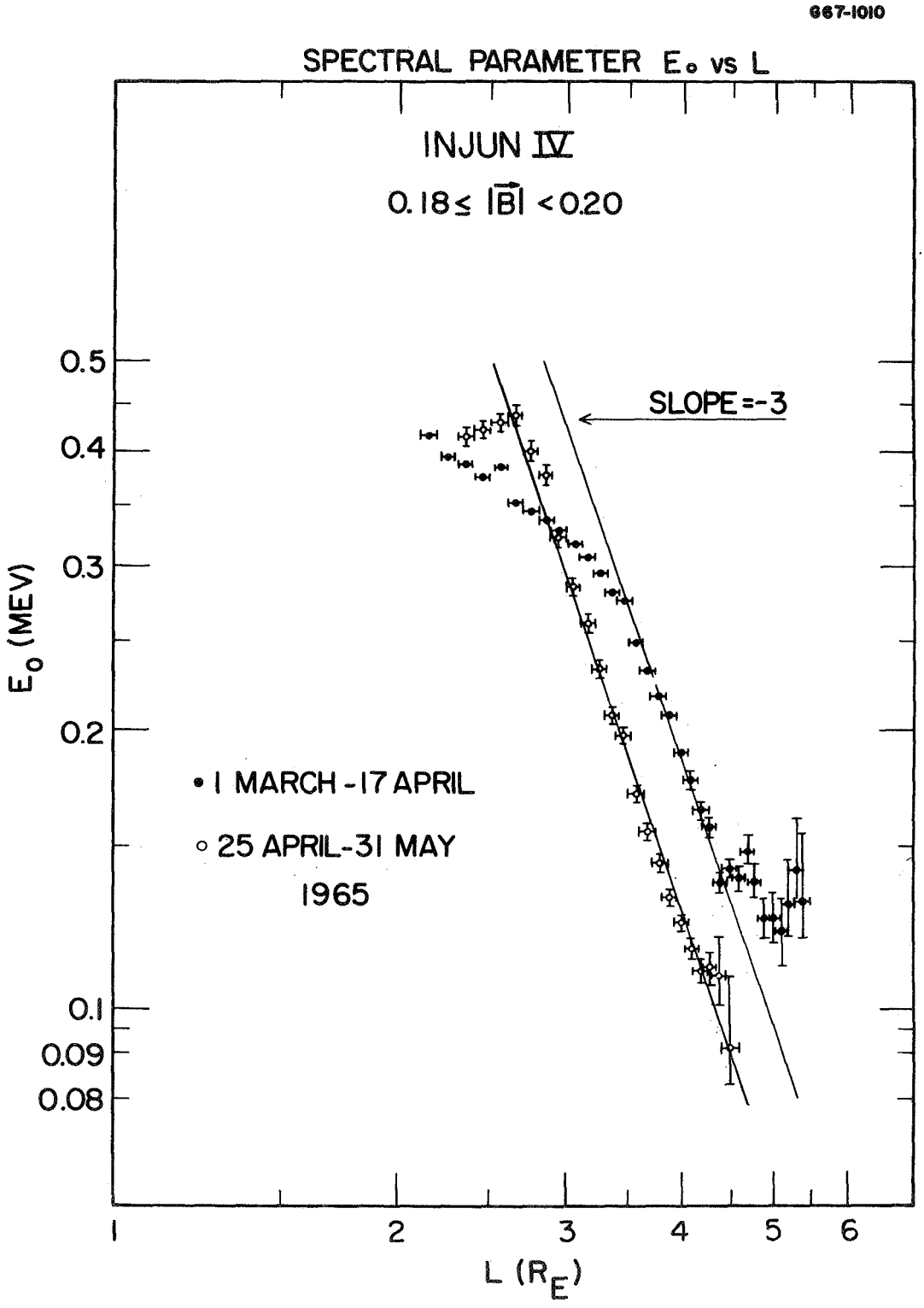
667-1010
SPECTRAL PARAMETER E₀ vs L
INJUN IV
0.18 ≤ |B| < 0.20
SLOPE = -3
• 1 MARCH - 17 APRIL
○ 25 APRIL - 31 MAY
1965
E₀ (MEV)
0.5
0.4
0.3
0.2
0.1
0.09
0.08
1
2
3
4
5
6
L (R_E)

Figure 17.

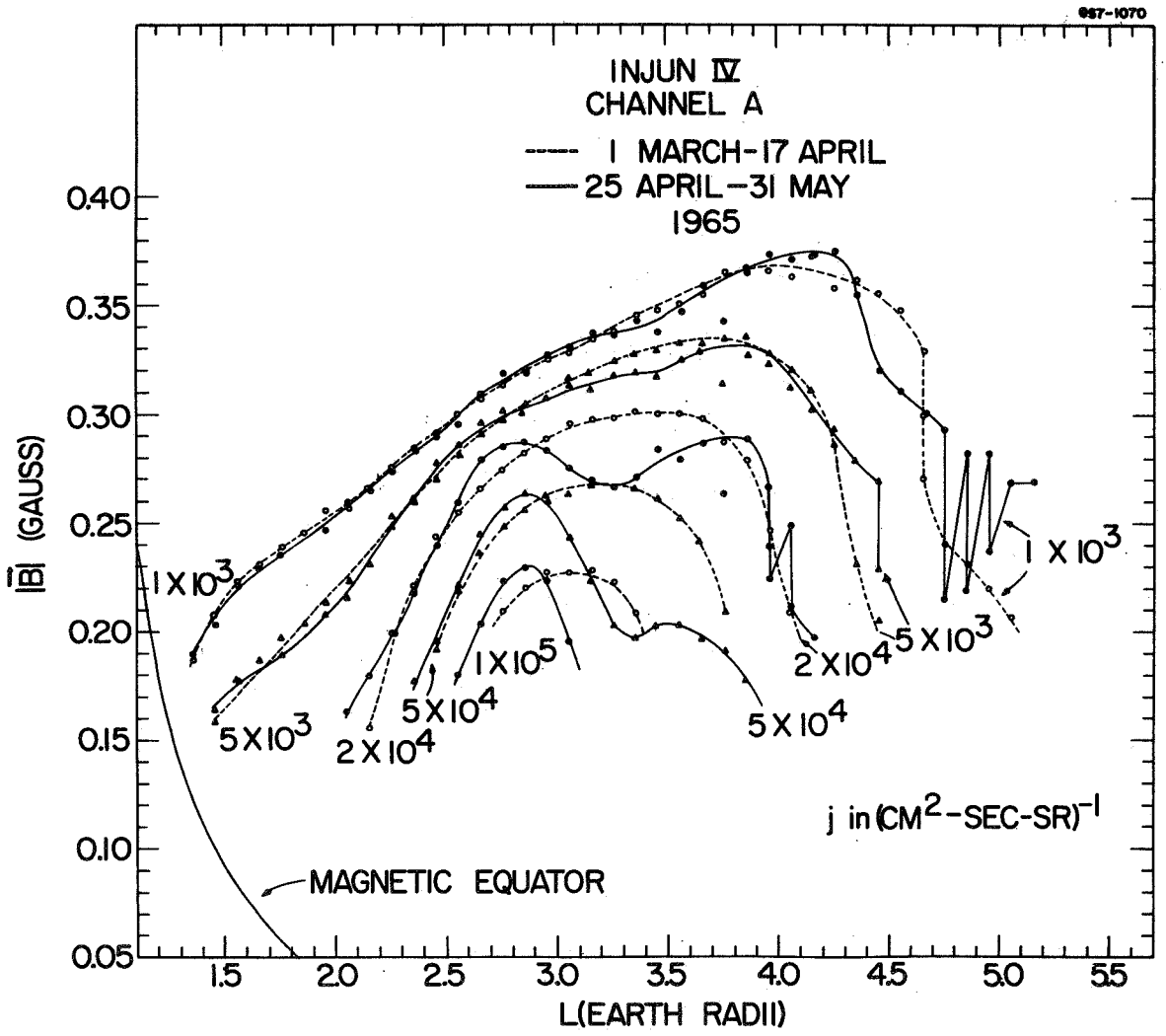
657-1070
INJUN IV
CHANNEL A
---- 1 MARCH-17 APRIL
—— 25 APRIL-31 MAY
1965
0.40
0.35
0.30
0.25
0.20
0.15
0.10
0.05
|B̄| (GAUSS)
1 X 10^3
5 X 10^3
2 X 10^4
5 X 10^4
1 X 10^5
5 X 10^4
2 X 10^4
5 X 10^3
1 X 10^3
j in (CM^2-SEC-SR)^-1
MAGNETIC EQUATOR
1.5
2.0
2.5
3.0
3.5
4.0
4.5
5.0
5.5
L(EARTH RADII)

Figure 18.

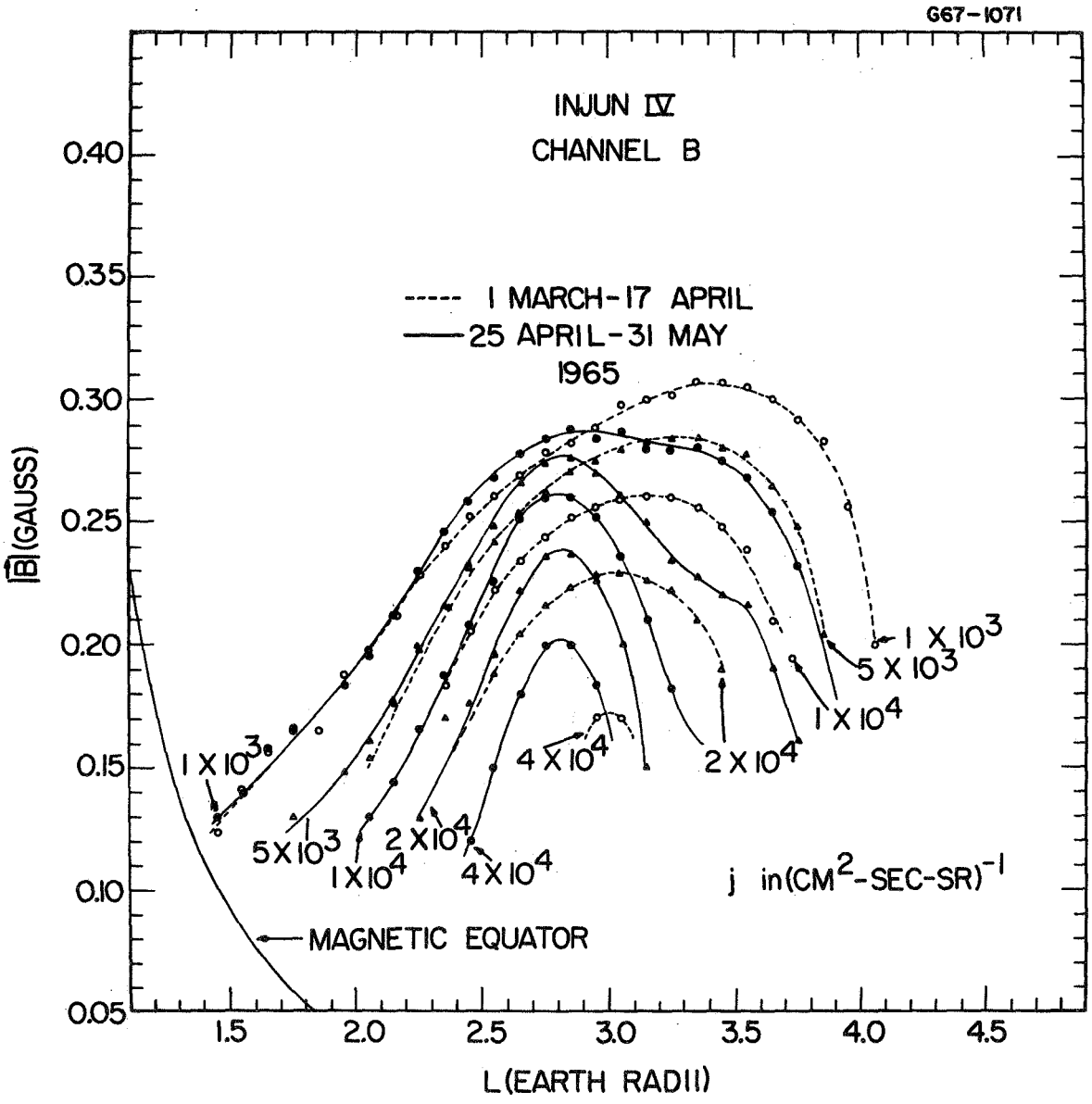
G67-1071
INJUN IV
CHANNEL B
----- 1 MARCH-17 APRIL
——25 APRIL-31 MAY
1965
|B|(GAUSS)
0.40
0.35
0.30
0.25
0.20
0.15
0.10
0.05
1.5
2.0
2.5
3.0
3.5
4.0
4.5
L(EARTH RADII)
1 X 10^3
5 X 10^3
1 X 10^4
2 X 10^4
4 X 10^4
j in(CM^2-SEC-SR)^-1
MAGNETIC EQUATOR

Figure 19.

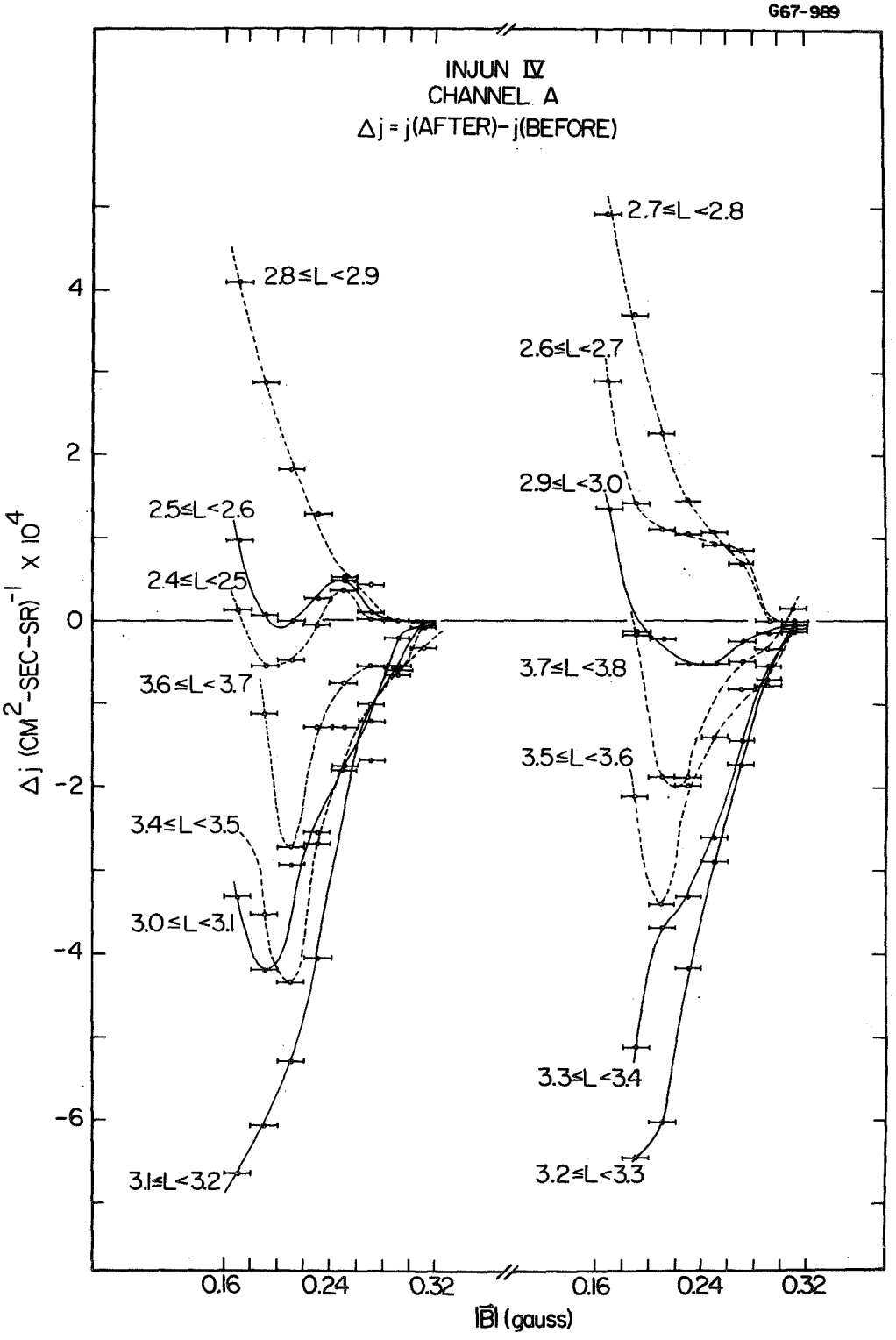
G67-989
INJUN IV
CHANNEL A
Δj = j(AFTER)-j(BEFORE)
2.7≤L<2.8
2.8≤L<2.9
2.6≤L<2.7
2.9≤L<3.0
2.5≤L<2.6
2.4≤L<2.5
3.7≤L<3.8
3.6≤L<3.7
3.5≤L<3.6
3.4≤L<3.5
3.0≤L<3.1
3.3≤L<3.4
3.1≤L<3.2
3.2≤L<3.3
Δj (CM²-SEC-SR)⁻¹ X 10⁴
4
2
0
-2
-4
-6
0.16
0.24
0.32
|B| (gauss)

Figure 20.